University of Nairobi

School of Mathematics

ISSN: 2410-1397

Master Project in Mathematics

Discontinuous Galerkin Finite Element method for solving Equations in Ocean Circulation

Research Report in Mathematics, Number 12, 2017

Mathias Nthiani Muia
I56/82837/2015

August 2017

Submitted to the School of Mathematics in partial fulfilment for a degree in Master of Science in Applied Mathematics

Discontinuous Galerkin Finite Element method for solving Equations in Ocean Circulation

Research Report in Mathematics, Number 12, 2017

Mathias Nthiani Muia
I56/82837/2015

School of Mathematics
College of Biological and Physical sciences
Chiromo, off Riverside Drive
30197-00100 Nairobi, Kenya

Master of Science Project
Submitted to the School of Mathematics in partial fulfilment for a degree in Master of Science in Applied Mathematics

Prepared for The Director
Board Postgraduate Studies
University of Nairobi

Monitored by: The Director
School of Mathematics
University of Nairobi

Supervised by: Dr Charles Nyandwi
School of Mathematics

Abstract

Fluid mechanics is a branch of mechanics that is concerned with the study of fluids, their properties and the effects of forces acting on them. It can be used to model a large number of fluid systems including the flow of water down the bathroom sink to the complex systems of ocean and atmospheric circulations. This project analyzes key components of the ocean circulation modeling and presents the physical and computational issues raised in numerical solution of equations generated in the study of shallow water flows in the earth's atmosphere. We describe ocean circulation into detail and outline the relationship between oceanic and atmospheric circulation. The ocean-atmospheric circulation discussed in chapter one is made to help us understand the effects of Ocean circulation on weather, climate and the global energy transfer. The main equations connected to ocean circulation (in a rotating framework) have been introduced and systematically modified by applying some standard approximations to obtain the so called shallow water equations (SWEs). SWEs, as example of hyperbolic system of partial differential equations, have been most of the time solved using the Finite Differences Method (FDM). Finite Element methods (FEM) and Finite Volume methods (FVM) have also been used. The 2D SWE representing oceanic circulation has not been solved in this work. At a later stage of this work, we derive the 1D shallow water equations which are free of the Coriolis parameter and the effect of rotation. This 1D SWE is then solved using the Discontinuous Galerkin Finite Element Method (DGFEM). The reason why we choose this method over the many numerical methods is because it combines the advantages of the FEM and FVM and seems to present well balanced solutions. In particular we use the Runge-Kutta DGFEM in finding our solution due to the following reasons:

1- Its ability to preserve the capability of the FEM of handling complicated geometries.

2- It increases the degree of approximating polynomials locally. This allows efficient p-adaptivity for each element independently.

3- Allows data communication only between neighboring elements. This gives room for an efficient parallelization.

Although recent advances on the DGFEM for the shallow water equations with topography source terms have been considered, we limit ourselves on the solution of one dimensional shallow water equations which are free of th Coriolis parameter and the effects of rotation. This choice is made so that we can easily illustrate the main advantages of this method especially if the dam break problem is concerned.

Dissertations in Mathematics at the University of Nairobi, Kenya.
ISSN 2410-1397: Research Report in Mathematics

DISTRIBUTOR: School of Mathematics, University of Nairobi, Kenya

Declaration and Approval

I the undersigned declare that this project report is my original work and to the best of my knowledge, it has not been submitted in support of an award of a degree in any other university or institution of learning.

Signature Date

Mathias Nthiani Muia
Reg No. I56/82837/2015

In my capacity as a supervisor of the candidate, I certify that this report has my approval for submission.

Signature Date

Dr Charles Nyandwi
School of Mathematics,
University of Nairobi,
Box 30197, 00100 Nairobi, Kenya.
E-mail: nyandwi@uonbi.ac.ke

Dedication

This project is dedicated to my family.

Contents

Acknowledgments

First and foremost, my gratitude goes to the Almighty God for granting all of us peace and good health to proceed successfully with this work.

Second, I would like to thank the University of Nairobi for offering me a scholarship which enabled me undertake my studies comfortably. I appreciate my lecturers in the department of Mathematics for equipping me with the knowledge to enable me face this work with ease.

I would also like in a more special way to thank my supervisor Dr. Charles Nyandwi for the hard work he did guiding me on all the aspects of this work to see that my work was of good quality. I could not have managed to come this far without his support.

Next I would like to pass my heartfelt gratitudes to my classmates, Kariuki D. Waweru, Jeniffer Chepkoril, Patrick Kamuri and Robert Makanga for being always there for me when I needed their assistance during this work.

Lastly, I would like to pass my sincere gratitude to my family for persevering the hardships I had to take them through during the accomplishment of this work. To all whom I have not mentioned here by name and contributed to my success, feel appreciated.

Mathias Nthiani Muia

Nairobi, 2017.

1 Introduction: Ocean circulation Modelling

1.1 Oceans and Ocean circulation

About two-thirds of the earth's surface is occupied by water bodies. The water bodies include oceans, seas, lakes, rivers, swamps artificial water reservoirs such as dams. In this project, we are going to study shallow water flows in these systems, study oceanic hydrodynamics and solve a one dimensional shallow water flow then apply the solution obtained to the dam break problem.

Oceans play a very important role in the global weather and climatic patterns. They act as a regulatory devices for the global climate, for instance by transporting huge amounts of heat from the tropical regions to the poles. During the process of ocean circulation, large amounts of energy are transported around the world. This is done by both surface and deep ocean currents which flow within the oceans like rivers; some currents are violent on their course whereas others are slow and meander along their course. Ocean circulation is caused by a combination of winds and variations in both temperature and salinity.
The movements of the earth especially its rotation play a very important role in dictating the paths taken by water masses during ocean circulation. Wind-driven circulation mainly occur within a region between the surface of the ocean and a depth of a few hundred of meters. Changes in temperature and salinity of the ocean water lead to variation in density which is a key factor contributing to massive water movements. Density-driven circulation is mainly dominant near the ocean bottom and takes place in form of "thermohaline" circulation. This is because it is caused by temperature differences and changes in salinity. Thermohaline circulation is also termed as "overturning" circulation and involves vertical water movements, whereby warm water flows towards the poles near the surface, at the poles, it gets cooled, sinks and flows back towards the equator in the interior. This form of circulation is very significant for support of aquatic life as convectional effect causes cold water from beneath to rise upwards to fill the gap left by the misplaced water a process called "upwelling". The upwelling part of thermohaline circulation is important as it brings nutrient-rich deep water up to the surface hence playing as a mode for supplying nutrients to ocean living organisms. Radiocarbon tests shows that this mode of ocean circulation turns over all the ocean water within periodic intervals of about 600yrs. This form of circulation transports about $10^{15}W$ of heat energy towards the poles hence playing a very crucial role in the earth's climatic changes.

Factors that influence ocean circulation

Temperature: This Ocean property is mainly dependent on the atmosphere which takes or adds heat on the surface of the water. Temperature differences in different layers of the ocean water influences circulation through convectional currents.

Salinity: This refers to the quantity of salts dissolved in the water. Sea water is composed of 3.5 percent salt with Sodium chloride being the most common salt. This property varies by small ranges in the surface zone. This variation is sufficient to affect water circulation.

Pressure: It is the effect of the weight of overlying water mass felt at a given depth. This property varies with depth. The atmosphere also exerts pressure on the water surface. Variation in pressure on the water layers may cause the density to change which in turn trigger density-driven ocean circulation.

Density: We define density as mass per unit volume. In water bodies, density increases with depth. It is dependent on temperature, salinity and pressure and its variation between two regions of the ocean trigger mass movements of water. In most models, density variations are usually ignored and eliminated by applying the Boussinesq approximation to obtain the so called Boussinesq equations.

In modeling of natural phenomena such as weather and climate, dynamics in both the oceanic and atmospheric systems are very important. This is because a lot of exchanges take place between these two including exchange of different forms of energy such as heat, exchange of moisture and water in the processes of evaporation and precipitation respectively. Due to these inter-relationships, we cannot talk about oceanic circulation without touching on atmospheric circulation.

1.1.1 General Atmosphere-Ocean circulation

Models of the ocean and the atmosphere deal with descriptions of circulations of heat, water, air and other components of these systems. In the circulations that take place in both systems, a lot of exchanges take place and this makes it possible to come up with a combined model design. A combined ocean-atmosphere general circulation is used to study the features of the ocean circulation and its impacts on the climate of the world (Toggweiler, 1994). This is achieved in a succession of global experiments and models that help predict the future changes in the climate resulting from effects of ocean circulation. The oceans play a very vital role acting as a storage site for heat to regulate seasonal changes in the atmosphere as well as act as a transport media, moving heat all over around the globe. Heat transported by the ocean is a very important component of the global heat budget, (Trenberth and Caron, 2001). Different ocean circulation models developed

by different researchers have been observed to come up with a fine detail.
Changes in the land surface configurations (topography) adjacent to the ocean coast causes variation in temperatures, winds and rainfall. This is because heat transports within the system are affected to some extend. Study indicates that if all the ocean transport was to be inhibited, it would lead to a reduction in the global mean of 8^oC, coupled with a sharpening of the meridional temperature gradient. This is because ocean transport is very important in in determining the global atmospheric humidity. The level of humidity (amount of water vapor in the air) determines the tropical albedo hence acting as a regulator of global surface temperatures.
The atmospheric and oceanic systems are complex ones, with processes and feedbacks that operate over timescales ranging from seconds to thousands of years and spacial scales ranging from millimeters to tens of thousands of kilometers. This complexity together with the inability to perform controlled experiments has led to invention of more sophisticated climatic and oceanic models e.g. Gordon et al. [2000]; Roeckner et al. [2003]; Marsland et al. [2003] which are climatic models capable of providing suitable feedbacks between components. However, due to the high costs of integrating these models, they are only appropriate for use in questions of the past, current and future climatic systems. To counter this, more general and simpler models are coming up for purposes of learning specific processes that function in our climatic systems. According to Broecker, (1985) and McManus, (2004), changes in the thermohaline part of ocean circulation are considered to have been very influential in the climatic changes that has been experienced over the earth's history.
The effects of changes in the ocean circulation and transport systems has been analysed in a number of studies. The first general ocean circulation model was developed by Stommel (1948) and Munk, (1950). They generated analytical models of wind-driven ocean circulation confined in rectangular basins. This they did by applying simplified dessipative laws. The first numerical ocean circulation models were developed by Bryan and Cox (1967) while the impacts of ocean circulation on climate were addressed later in time with the development of coupled atmosphere-ocean circulation models.
The strong interdependence between ocean circulation and the climate means that a model designed to predict climatic changes must include aspects of ocean circulation and mixing as well as aspects of atmospheric circulation plus the physics of weather factors.

1.1.2 Numerical ocean Modelling

Numerical ocean modelling entails computational techniques that describes mathematically aspects of the ocean. It is important in making predictions of ocean processes to some points in the future. It gives a convenient way of mathematically representing phenomena connected to this complex geophysical system. Oceanic models are used widely by oceanographers and weather/climate scientists as experimental tools. With great improvements in the understanding of ocean models together with development in related computer programs, we can today model very realistic ocean fluid dynamics

representations.
Today this field is growing rapidly due to its many applications. Some of the applications of ocean model design include; studies of climate change, oceanography and ultra-refined resolution process studies. The challenge being faced today by developers is that of code distinctions which prevents mathematicians from interchanging algorithms. This makes it difficult to compare simulations directly or reproduce them using different codes hence increasing burdens of model design maintenance.
Numerical ocean modelling involves solving geophysical fluid dynamics equations. Different modelers take different approaches to represent the ocean fluid dynamics i.e. in terms of the model equations and the method used to solve them. The type of model also depends on the aspect of the ocean being modeled. Models such as Dale B. Haidvogel, John L. Wilkin and Robert young (1988) use the complete primitive equations with sigma-vertical coordinates to study regional and basin-scale ocean circulation processes. This is just an example which presents just a grain of sand in the desert in terms of models that are 3-dimensional.
Many modelers have made modifications on the complex original 3D equations to obtain forms of equations that best suits their area of study. An example of modified equations is the shallow water equations which are simplifications of the 3-D set of equations containing the Navier-Stokes equations, equations representing tracer distribution and the equation of state. Oceanic wave modelling for waves that have large wavelengths is done using the shallow water equations (E. Hanert, V. Legat and E. Deleersnijder, 2002). Models are usually associated with partial differential equations called primitive equations which have to be solved at the end. To solve the final model equations three numerical methods have been used in the history of oceanic-atmospheric modelling, namely; the finite difference methods (FDM), Spectral methods (SM) and the finite element methods (FEM). Using these solutions, approximations are then made to interpret the properties of flows in the ocean. Manipulations are done on the obtained equations mainly through integrations over the ocean depth to obtain other forms of the equations known as Shallow water equations.
Modeling practices are usually associated with a wide range of difficulties. The modeler is faced by challenges of making decisions on the choice of the numerous approaches that can be undertaken to accomplish the task of modelling. The section below presents the physical and computational issues encountered in oceanic modeling.

1.1.3 Physical and computational issues in numerical ocean circulation modelling

The process of modeling involves physical, mathematical and computational aspects that has to be handled in order to arrive at the final results and conclusions. The modeler has to make decisions on;

a). The choice of scales (time- and spatial scales)

The ocean basins are thousands of kilometers in width and length. Circulations here present themselves in a wide range of time, space and mixing scales. The choice of the time- and spatial-scales has a significant effect on the numerical scheme to be used to model them.

b). choice of vertical coordinates

The depth of the ocean varies with some regions having depths of up to 5kms in average. The dominant form of circulation in the vertical is the thermohaline circulation. Vertically, the scale is normally very small compared to the horizontal scale, a property known as shallow water condition . In such flows the vertical accelerations of the fluid are negligible implying an hydrostatic nature of the fluid. Most of the flows that take place on the surface of the earth are shallow water flows. .

Traditional vertical coordinates can either be geopotential, terrain-following, isopycnal, hybrid or pressure coordinates. The terrain-following coordinate is suitable for representing an irregular bottom topography. Isopycnal coordinates are commonly adopted for idealized adiabatic simulations. They are widely used in global climate based simulations especially in a combination with the pressure coordinates. The hybrid coordinates are used in models aimed at generalizing vertical coordinate formulation. They allow other different vertical coordinates to be fixed depending on the model application and the fluid regime hence providing a specific area to work on for their next development.

c). Acoustic modes and gravity waves

The shallow water equations are linear in nature and this allows the existence of a large assortment of waves that are seen in the large scale circulation of the ocean. These waves are characterized by wavelengths which are long relative to the ocean depth and can be classified as **external** or **internal waves**. Waves that can be supported by a fluid in a rotating framework include the **inertia-gravity**, **Kelvin** and **Rossby waves**. Rossby waves, also called planetary waves are created by variation of the Coriolis parameter or by changes in the elevation of the bottom floor They greatly contribute in the development of large scale circulations of the ocean. Gravity waves on the other hand are generated by gravity and they are much faster than the Rossby waves.

Kelvin waves are caused by a combination of variation of the Coriolis parameter and the existence of dynamical boundaries. They have a minor impact on the general ocean circulation as they transport very small portions of the total ocean energy budget.

d). Assumptions

Valid assumptions and approximations on the original equations have to be considered. These approximations help to simplify the equations by eliminating acoustic modes and linearizing non-linear terms. The approximations used include; Boussinesq approximation, hydrostatic approximation, Newtonian fluid approximation and the spherical geopotential. The approximations used in this work are discussed in the next section.

e). Rotation of the earth

The geopotential approximation assumes that the earth is spherical, (Hanert, 2004) and in constant spinning about its axis, a movement called rotation. The effects of a rotating framework of reference on the equations of motion must be put into consideration during derivation of the primitive equations. The earth's rotation vector is defined by $\hat{\Omega} = \Omega\hat{k}$ where $\hat{k} = \cos\theta\hat{e}_y + \sin\theta\hat{e}_z$ is a unit vector along the rotation axis of the earth. The Coriolis acceleration is given as

$$2\Omega \times \hat{v} = f_*\hat{e}_y \times \hat{v} + f\hat{e}_z \times \hat{v}$$

where $f = 2\Omega\sin\theta$ is known as the Coriolis parameter and $f_* = 2\Omega\cos\theta$ is the reciprocal of the Coriolis parameter. We also assume the gravitational acceleration, g to be constant.

f). Mixing scales

A major part of oceanic flows is involved with the transport of tracers such as temperature, salinity and other biochemical species. Temperature and salinity directly affects density of the ocean water and hence influence the dynamics of the oceans. These two are classified as active tracers while the other tracers which have less influence on the dynamics of the fluid are called passive tracers.

Tracer concentration is affected by the convergence of tracer flux plus the potentially non-zero sources or sinks. Alternatively, tracer concentration may be caused to vary by the mixing caused by small-scale turbulent motions having lengths as small as just a few centimeters. The full extend of these small-scale motions in the ocean model is parameterized by use of some diffusion operator to outline their large-scale effects.

On the surface layer, the tracer concentration keeps on changing as a result of; addition of fresh water from rivers and precipitation and heat exchange with the atmosphere. The process of balancing tracer concentration is a continuous one. This is achieved via diffusion and oceanic fluid movements (both horizontal and thermohaline circulations).

g). The governing equations

Some physical and computational challenges are encountered during the simulation. The oceanic general circulation includes the horizontal and vertical transport of water, heat, air, salts and other biogeochemical species. All these components of the ocean are involved in establishing the dynamical balances in the oceanic systems. The circulation therefore includes associated pressure, salinity and temperature fields which influence currents through the density variations. Due to the rapid growth of this field, alot of time and resources are being devoted to research activities. Many questions arise during the design of models with some remaining partially answered while others remain completely unanswered. These fundamental questions give the motivation to mathematicians, physicists and oceonographers to venture in studies in these fields so as to come up with valid answers. Ocean circulation is normally described by the Navier-Stokes equations sed in a rotating framework plus the equations relating conservation of tracer deposits and

the equation of state. These are the equations that modelers aim to discretize and most of the questions asked in the field of ocean circulation modeling are connected to these equations. The questions to answer include;

- The question of whether the equations used in the model should be hydrostatic or non-hydrostatic? The model of Marshal et al. (1997) states that both forms of models are equally sufficient.
- Should the fluid flow be taken to be compressible or should it be incompressible? Incompressibility of the fluid is achieved by applying the Boussinesq approximation (discussed later in this chapter). Some modelers today are opting to use non-Boussinesq fluid conditions in their work to represent sea level changes due to steric effects, Griffies (2004); Marshall et al. (2003); Lorsch et al. (2004).
- Another dilemma encountered is whether to consider the upper free surface of the ocean as non-varying in time (Bryan [1969]) or should we allow it to fluctuate naturally due to water motions? A fluctuating/varying surface puts into consideration the effects of addition of fresh water onto the surface and lose of water in form of water vapour into the atmosphere.
- After selecting the model equations known as primitive equations, the question of the choice of vertical coordinates to be adopted arises. We have a wide range of vertical coordinates to choose from which include terrain-following sigma coordinates, geopotential coordinates, isopycnal coordinates and the generalized hybrid coordinates.
- Which horizontal grid system should be used? In the solution of the primitive equations, we have to discretize the domain using horizontal grids. Some of the commonly used grid systems are the traditional A, B, C, D and E grids of Arakawa and Lamb (1997), the spectral methods discussed by Haidvogel and Beckmann (1999).
  Numerical methods are very important for time-stepping the ocean forward. The numerical methods used include, Finite volume methods (FVM), Finite difference methods (FDM), Finite element Methods (FEM), Continuous/Discontinuous Galerkin Finite Element Method and spectral methods

As a result of all these issues associated to ocean circulation models, specific accurate approximations and assumptions are applied to reduce the original equations to simpler forms. In this work, we choose to modify our original equations into the shallow water equations (SWE). We begin with the continuum equations of hydrodynamics expressed in a rotating framework and reduce them to the shallow-water equations form. This way of connecting from the 3D hydrodynamics equations to 2D SWEs also helps us avoid the difficulty encountered solving the full 3D equations. SWEs are suitable for modeling

waves in the atmosphere, rivers, lakes, dams, oceans and seas that have large wavelengths compared to the depth of the water basin. They are applied in models of Rossby and Kelvin waves and under some conditions the gravity waves. SWEs are used to model tides which have very large wavelengths of roughly up to 100 kilometers. Hence the very deep ocean may be assumed to be shallow when it comes to tidal motion since the depth is much smaller than the tidal wavelength.

In this work we choose the shallow water type of model since our work is to the larger extend based on ocean circulation that involve oceanic waves such as the Kelvin and Rossby waves which display very large wavelengths. In their linearized form the shallow water equations still display the main features of these waves. The acoustic waves are eliminated by making the flow incompressible. This is done by applying the Boussinesq approximation which assumes that no density variations in the fluid. The acoustic/sound waves make use of compressibility of the water and are very fast to be relevant for geophysical flows. The incompressibility of the flow implies non-divergence and we call this type of flow **barotropic** (flow with no density variations). The only driving forces in these flows are the gravity and Coriolis force and the waves propagated in this kind of flows are the Kelvin and Rossby waves. The type of shallow water equations on which our model will be based takes the form given below. The derivation of these equation is done in chapter 3. The 2-D SWE derived in chapter 3 is not solved in this work, it has been left to be solved in further work.

2 Background of the problem

The origin of the shallow water equations dates back to the mid 19^{th} century. The concept of shallow water flows was first initiated by a French mathematician and mechanician, **Adhemar Jean Claude Barre de Saint-Venant** (1797-1886). He contributed significantly in the initial stress analysis and developed the unsteady open channel flow shallow water equations (also known as the **Saint-Venant equations**).

With the advancement of computational technology, many applications of these equations have mushroomed in different disciplines. For instance, they are used in modeling of oceanographic and atmospheric fluid flows to design models that describe phenomena in these systems. For example, modelers have come up with designs that help in prediction of climatic changes, spread of pollutants polar ice-cap melting, e.t.c to mention but a few. With the growing interest of research in the fields of oceanography and atmospheric studies, different researchers have come up with shallow water models that suit different purposes. Dronkers (1964) describes the use of shallow water equations to determine ocean circulation patterns and tidal elevations at the interior of an enclosed region subject to tidal waves. Kahawarn (1978) proves the relevance of the shallow water equations in the prediction of tsunami waves which are known for causing severe flooding destruction of property and loss of lives. Research being still active in this field, mathematicians, physicists and oceanographers are still seeking for the possibility of using these equations to model schemes that would be useful for conversion of tidal energy into commercially utilizable forms. Attempts in this interesting field are outlined in the works of Charlier (1982) and Gray and Gashaus (1972). Leendertse, 1967, used SWEs model to describe the effect of waves originating from explosion of military nuclear bombs near ocean surfaces or in the interior of the ocean water.

The numerical solution of shallow water equations was among the first numerical simulations to be carried out on digital computers during their invention in the 1950's. Hensen, (1956) used computational power to model oceanographic flows using SWES while Charney et al. (1950) modeled atmospheric flows.

All authors and/or researchers have arrived to the SWES through successive approximations of the general equations governing fluid motions. These general equations are normally the well-known Navier-Stokes equations plus the equations of conservation of tracer deposits (heat, salt and biogeochemical tracers) and the equation of state. Several numerical methods have been applied to solve the final exact form of the SWES with the mostly used method being the Finite Difference Method (FDM). Hanert (2004) in his PHD thesis uses the FEM with unstructured grids to arrive at quite nice results. Other methods which have been applied to solve these equations include the Riemann solver for SWES (J. Bohacek [2015]; L. George [2004]; D. Ambrosi [1995]), the collocated coupled solution

method (CCSM) used by Aukje de Boer (2003). There are several more methods which have been proved to give very accurate solutions.
In this work, we use the Discontinuous Galerkin Finite Element Method to solve the one-dimensional shallow water equation for a flow through a channel.

2.1 Problem statement

Our main task in this project is to study and understand the numerical methods of solving SWEs and specifically apply the Discontinuous Galerkin finite element method to solve the 1D SWE;

$$\partial_t \mathbf{u} + \partial_x f(\mathbf{u}) = s(\mathbf{u})$$

subject to initial conditions defined by a dam channel domain:

$$h(x,0) = \begin{cases} h_L, & \text{if } 0 \leq x \leq 300 \\ h_R, & \text{if } 300 < x \leq 1000 \end{cases}$$

$$u(x,0) = 0 \qquad 0 \leq x \leq 1000$$

This equation is the conservation law form of the 1D SWE derived in chapter 3.

2.1.1 Main objective

To study and understand Shallow water flows, translate the dynamics mathematically into equations and use these equations to come up with a model that can be of importance in the societies in which we live.

2.1.2 Specific objectives

1. To study and understand fluid flows on the sphere and relate the flows to the shallow water equations.
2. To apply the SWEs to model flows in a channel.
3. To study and understand the FEM and the DG finite element method for solving PDEs.
4. To apply step-wise DG formulation to the 1D-SWE to determine its numerical solution.

2.2 Applications of SWEs

Shallow water flows are experienced in oceans, rivers, coastal estuaries, lakes and the atmosphere. In addition to ocean circulation modeling the shallow water equations have many more practical applications in different disciplines. These include;

i. In oceanography to determine tsunami-wave propagation and prediction of tidal currents. This is important for navigation purposes in seas and oceans and prediction of disasters.

ii. Analysis of the dam-breaking problem and the associated flood elevation.

iii. Determination of pollutant dispersion and storm surges.

iv. In meteorology and atmospheric flows to predict weather and climatic changes.

v. Planetary flows (Vreugdenhill, 2004) and internal flows.

2.3 Literature review

Rigorous research has been undertaken in the study of oceanic and atmospheric circulations. Different numerical models that describe the dynamics in these complex geophysical systems has been on the growth for the last over 50 years.
The first model of ocean circulation was designed in the 1900's after Ekman, (1905) described the effects of the rotation of the earth on oceanic currents. Sverdrup, 1947, described the effects of rotation on wind-driven currents. He came up with a simple law governing this relation. However, these initial models were non-numerical, they formed a basis for the development of modern numerical models. Bryan and Cox, (1967) combined the very first numerical ocean circulation model. Since their pioneering, models that aim at predicting different physical phenomena have been on the rise. Haidvogel and Beckmann, (1999), give a more detailed overview of the numerical modelling.
Dale B. Haidvogel, (1991) uses spectral methods with vertical sigma coordinates and orthogonal curvilinear horizontal coordinates to solve the full equations of ocean circulation. His model becomes very efficient for irregular basin geometries with non-uniform bottom topography.

Bernard Bernier, Patrick Marchesiello, Anne Pimenta and Macky Coulibaly, (1995) describes the terrain-following $\sigma-$coordinates numerical model for a case study of circulation in the south Atlantic. Their model is of the semi-primitive type-a model introduced by Haidvogel et al., (1991). In this work, they investigate the advantage of $\sigma-$coordinates in the calculation of pressure gradient and the diffusion of tracers. They make use of open boundary conditions based on radiation conditions and climatology relaxation.

Haidvogel and Beckmann, (1999) ocean model give a good description of the general ocean circulation. They present 3-D ocean models using the Modular Ocean Model (MOM) approach, Spectral coordinate models (SPEM), Miami Isopycnic Model (MICOM) and Spectral Element Ocean Model (SEOM). They give detail applications of each of these types of models and proceeds to give a case study on the North Atlantic ocean model using the SPEM approach.

Many authors and researchers have made use of the Finite Difference Method (FDM) and the Finite Volume Method (FVM). Quing Wang, (2007) describes a FEM ocean model and its aspect of vertical discretization. He concentrates mainly on the study of the performance of different vertical grids by using a couple of numerical experiments based on the FE ocean models. He also develops a new version of a Finite Element Ocean circulation Model (FEOM). The horizontal span in his work is based on unstructured triangular element grids and prismatic grids in the vertical sense. He makes use of continuous linear equations to describe the horizontal aspects such as velocity, temperature and salinity. The standard set of hydrostatic primitive equations are solved with the characteristic based split (CBS) scheme which is used to suppress computational pressure modes.
The FE method has not been used as widely as the FD method. Since the use of this method by Fix (1975), the most applications of the FE method has been mainly on the coastal and shelf regions. Fix described the nice properties of this method in his early work-the methods gives a natural treatment of boundaries and has the property of energy conservation which is a very important aspect of these methods. The most renown oceanic models that apply the FE method are Lynch and Gray, (1979); Lynch et al. (1996); Platzman, (1981); Le Provost et al., (1995); Le Roux et al. (1998); Walters, (2008) which all focus on on coastal and shelf region modeling. Some finite element models also deal with stationary-state ocean inverse problems (Brasseur, [1991]; Schlichtholz and Houssais [1999]; Dobrindt and Schroter [2003] and Losch et al. [2005]). A combination of of the FEM and unstructured grids gives a very fine detail of resolution (Danilov et al. [2004]; Ford et al. [2004], Hanert [2004] and White et al. [2007]). The FEM in general becomes more accurate on unstructured meshes (Hanert, 2004). The FEOM supports a couple of vertical grids namely z-level, sigma and $z+\sigma$ grids but it does not support isopycnal grids. Until present, there are only a few 3D FE ocean circulation models whereby of all these none of them has been designed for large-scale ocean circulation on decadal time scales. The most commonly used models are QUODDY (Lynch and Naimie, 1993) and ADCIRC which apply FE method discretization only in the horizontal direction and they are designed for tidal and coastal applications within relatively short time periods (just a number of months). Sergey Danilov, Gennady Kivman and Jens Schroter, (2002) describes a 3D FE ocean model for investigating the large scale ocean circulation on time-scales from years to decades. In their model they solve the primitive equations in the dynamical part and the advection-diffusion equations for temperature and salinity in the thermodynamical part. Their model makes use of linear functions to represent horizontal velocities on the tetrahedra used in the 3D mesh. The tracers on the tetrahedra and the surface elevation on the surface triangles are also represented using linear functions.

Another form of models in this field is the Shallow water modelling. These models are a simplification of the real world whereby the ocean is represented by a single layer of fluid of a varying height and a constant density. SWE models have been widely developed for different applications such as modeling tidal currents, modeling the problem of dam-break (Robert Brandoni and Gerald Freitas, 2012). Other works that make use of SWEs

to model dam-break problems include Szu-Hsein Peng (2012), C. Ancey, R. M. Inverson, M. Rentschler and R. P. Denlinger, (2008). Hossam S. Hassan, Khaled T. Ramadan and Sarwat N. Hanna, (2010) uses the FEM to solve 2D ocean model equations. The work out rigorous calculations by employing fractional steps in the numerical procedure to obtain the solutions.

Our current study involves solution of 1D SWEs for modeling a flow with a uniform cross-section. We use a practical problem of a dam with a rectangular cross-section to test our results. The method we use to solve the equations is aimed at improving the resolution. We aim to obtain very accurate solutions that can be interpreted and applied in risk management in case a dam fails.

3 The shallow water equations

The SWEs representing ocean circulation contain the effects of rotation of the earth. They cater for centrifugal forces and effects of gravity. They are linear equations and can be represented on a plane (in two dimensions). The two-dimensional shallow water equations interprets properties and effects of shallow flows under specified initial and boundary conditions. The basic equations that govern the dynamics of fluids are built on the principles of conservation of mass, momentum and energy which are well represented in the Navier-Stokes equations. Due to the nature of ocean/sea water, these equations together with equations of conservation of heat, salt and the equation of state are used to represent oceanic fluid dynamics. These initial equations are non-linear in many terms and they support fast acoustic modes making them both difficult to solve and costly to work with. We apply a series of approximations and assumptions to these equations to simplify them to the primitive equations which are then used in the model. The general equations in a rotating framework are given by

$$\frac{\partial(\rho\vec{v})}{\partial t} + \nabla.\rho\vec{v}\vec{v} + 2\vec{\Omega} \wedge \rho\vec{v} + g\rho\hat{k} + \nabla p = \nabla.\tau \tag{1}$$

$$\frac{\partial\rho}{\partial t} + \nabla.\rho\vec{v} = 0 \tag{2}$$

$$\frac{\partial(\rho S)}{\partial t} + \nabla.\rho S\vec{v} = 0 \tag{3}$$

$$\frac{\partial(\rho T)}{\partial t} + \nabla.\rho T\vec{v} = \frac{1}{c_p S}\nabla.\mathscr{F}_T \tag{4}$$

$$\rho = \rho(T, S, p) \tag{5}$$

where as described previously,
ρ is mass density , $\vec{v}$ velocity , p the pressure , S represent the salinity ,
T the potential temperature which add up to 7 independent variables while
$\vec{\Omega}$ is the rotation vector of a sphere, g the gravitational accceleration and c_p
the specific heat capacity at a constant pressure τ is the stress tensor and $\mathscr{F}_T$
represent non-advective heat fluxes

Eq (1) and (2) represent the Navier-Stokes equations of expressed in a rotating framework of reference. Equations (3) and (4) relates conservation of tracer deposits, while the last equation, (5) is known as the equation of state.
Acoustic modes arise from the dependence of the density on pressure. These modes are very fast and are not of any importance in geostrophic fluid flow and they can be eliminated from the equations.

Sound waves

Using the equation of continuity, (2), we can write

$$\frac{D\rho}{Dt} = -\rho\nabla.\vec{v} \tag{6}$$

where $\frac{D}{Dt} = \frac{\partial}{\partial t} + \vec{v}.\nabla$ stands for the material derivative and $\nabla.$ is the divergence. Also using the chain rule to differentiate the equation of state (5), we obtain

$$\frac{D\rho}{Dt} = \frac{\partial\rho}{\partial T}|_{S,p} D_t T + \frac{\partial p}{\partial S}|_{T,p} D_t S + \frac{\partial\rho}{\partial p}|_{T,S} D_t p \tag{7}$$

where using Eq (6) and Eq (7) to eliminate $D_t p$ we can write for adiabatic motion;

$$\frac{1}{c_s^2} D_t p = -\rho\nabla.\vec{v} + \rho\lambda D_t T - \rho\gamma D_t S \tag{8}$$

with c_s, λ and γ (all functions of T, S and p) respectively representing sound speed, thermal expansion and the coefficient of haline expansion. This equation in its linear form together with the equations of momentum in linear form describes sound waves;

$$\bar{\rho}\,\partial_t\vec{v} = -\nabla p$$
$$\partial_t p = -\bar{\rho} c_s^2 \nabla.\bar{v}$$
or
$$\partial_{tt} p = c_s^2 \nabla^2 p$$

These waves travel at an average speed of $1500 ms^{-s}$ in water which translates to $100 km$ of distance they cover in a minute. This is unpractical for ocean scale calculations and therefore it is necessary to filter the equations of these acoustic modes by removing density dependence on pressure. This is achieved by making the approximations discussed below

Boussinesq approximation

This approximation assumes that the density is constant throughout the domain Ω except where gravitational body forces are involved. Thus $\frac{d\rho}{dt} = 0$. Using this we can represent the water density as a sum of some constant density and a smaller time- and spatial-varying perturbation;

$$\rho(x,y,z,t) = \rho_0 + \hat{\rho}(x,y,z,t)$$

where $\hat{\rho}(x,y,z,t) \ll \rho_0$ is a space- and time-varying term. Boussinesq approximation states that we may ignore $\hat{\rho}$ at all points except when gravitational forces are involved. As a result the equation of mass conservation (2) reduces to an equation of volume conservation

$$\frac{\partial u}{\partial x} + \frac{\partial v}{\partial y} + \frac{\partial w}{\partial z} = 0$$

In this case we call the flow incompressible. This kind of approximation helps us to linearize terms involving products of density with other dependent terms. For example $\rho\vec{v} \longrightarrow \bar{\rho}\vec{v}$ where $\bar{\rho}$ is the background mean, a scalar. With this approximation and assuming that the flow is non-divergent, the equations (1) to (5) are modified to the non-hydrostatic Boussinesq equations below

$$D_t\vec{v} + 2\vec{\Omega} \wedge \vec{v} + \frac{g\rho\hat{k}}{\bar{\rho}} + \frac{1}{\bar{\rho}}\nabla p = \frac{1}{\bar{\rho}}\nabla.\tau \tag{9}$$

$$\nabla.v = 0 \tag{10}$$

$$D_t S = 0 \tag{11}$$

$$D_t T = \frac{1}{\bar{\rho}c_p S}\nabla.\mathscr{F}_T \tag{12}$$

$$\rho = \rho(T,S,z) \tag{13}$$

This new system of equations does not support acoustic modes. These equations are however not easy to solve as they are prognostic in three components of velocity. We simplify these equations further by make the hydrostatic approximation.

Hydrostatic approximations

From equation (9) the vertical component of the modified Boussinesq momentum is given by

$$\frac{Dw}{Dt} + 2\Omega\cos\phi v + \frac{g\rho}{\bar{\rho}}\frac{\partial p}{\partial z} = \frac{1}{\bar{\rho}}\nabla.\tau^w$$

Using the fact that the horizontal scale is large compared to the vertical one, we can show that the vertical pressure gradient may be given as a product of the density and gravitational acceleration. The dominant balance from a scaling for each term is

$$\frac{\partial p}{\partial z} = -g\rho$$

We use the boundary condition $p = 0$ at $z = \eta$ (where $z = \eta$ is the surface elevation at the top) to obtain the internal pressure

$$p = \int_z^\eta g\rho dz$$

Let $z=-H(x,y)$ be the length of the water column from some fixed level $z=0$ to the bottom and $z=\eta(x,y,t)$ be the height from $z=0$ to the surface of the fluid as shown in. Integrating the non-divergent continuity equation vertically using the limits $-H\leq z\leq \eta$

$$\int_{-H}^{\eta}\partial_z w dz=[w]_{-H}^{\eta}=-\int_{-H}^{\eta}\nabla_h.\vec{v}_{hdz}$$

using the Leibniz's rule

$$\int_{-H}^{\eta}\nabla_h.\vec{v}_h dz=\nabla_h.\int_{-H}^{\eta}\vec{v}_h dz-\vec{v}_h|_{z=\eta}.\nabla_h\eta+\vec{v}_h|_{z=-H}.\nabla_h(-H)$$

The vertical normal velocity into the solid bottom is given by

$$w|_{z=-H}=w(-H)=-\vec{v}_h.\nabla_h H$$

At the free surface, fluctuations of the fluid are dominant and the rate of variation of the surface elevation with time is given by

$$\frac{D\eta}{Dt}=w|_{z=\eta}+(P-E)$$

where $\frac{D}{Dt}=\frac{\partial}{\partial t}+\vec{v}.\nabla$ is the material derivative and $-(P-E)$ is the excess evaporation over addition of water on the top surface. We can therefore write the free surface equation as

$$D_t\eta+\vec{v}_h.\nabla_h H=-\nabla_h.\int_{-H}^{\eta}\vec{v}_h dz+\vec{v}_h|_{z=\eta}.\nabla_h\eta-\vec{v}_h|_{z=-H}.\nabla_h(-H)+(P-E)$$

or

$$\frac{\partial\eta}{\partial t}+\nabla_h.\int_{-H}^{\eta}\vec{v}_h dz=(P-E)$$

This is the hydrostatic equation of continuity. The equations (1) to (5) then reduce to a new set of equations of the form

$$D_t\vec{v}_h+f\hat{k}\wedge\vec{v}_h+\frac{1}{\bar{\rho}}\nabla_h p=\frac{1}{\bar{\rho}}\nabla.\vec{\tau}_h \tag{14}$$

$$p=\int_{-H}^{\eta}g\rho dz \tag{15}$$

$$\partial_z w=-\nabla_h.\vec{v}_h \tag{16}$$

$$D_t S=0 \tag{17}$$

$$D_t T=\frac{1}{\bar{\rho}c_p}\nabla.\mathscr{F} \tag{18}$$

$$\rho=\rho(T,S,z) \tag{19}$$

$$\partial_t\eta=-\nabla_h.\int_{-H}^{\eta}\vec{v}_h dz+(P-E) \tag{20}$$

where $\nabla_h = \frac{\partial}{\partial x}\hat{e}_x + \frac{\partial}{\partial y}\hat{e}_y$ is the horizontal gradient operator, $\vec{v}_h$ is the horizontal kinematic eddy viscosity. Equations (14) to (20) are the **hydrostatic primitive equations (HPEs)**. These are equations for variables $u, v, w, p$and ρ together with the turbulence closure schemes for the diffusion and viscosity coefficients. The HPEs form the basis for most ocean general circulation models. Eq (14) represents the horizontal momentum, (15) is an equation of hydrostatic balance, (16) represents the vertical variation of motion, (17) to (19) represent distribution of tracers and the last equation is the hydrostatic equation of continuity. Equations (15), (16) and (19) are diagnostic one for each of ρ, p and w while equations (14), (17), (18) and (20) are prognostic and describe baroclinic or three-dimensional evolution. The four prognostic equations corresponds to a pair of gravity modes, a geostrophic mode (Rossby waves) and a thermo-haline mode. The free surface equation couples with the depth-integrated momentum equations to give a pair of external gravity modes and an external Rossby mode. We will derive the shallow water equations from further simplification of the HPEs.

Coordinate System

The equations we are dealing with are two dimensional. We therefore choose a 2D coordinate system called the β-plane coordinate system. In this system the $x-, y-$ plane is considered to be tangent to the earth at the latitude under consideration. The $x-$axis is taken to be in the direction of the latitude at that point whereas the $y-$axis is taken to be in the direction of the longitude. The $z-$axis is taken to be in the direction of the outward normal to the Earth's surface. The domain under consideration is the ocean and we denote it by Ω and the boundaries of this region by $\partial\Omega$.

Boundary conditions

The boundary $\partial\Omega$ of the domain includes the open/closed vertical surfaces that encloses Ω, the free surface and the impermeable bottom of the domain. The free surface is given as

$$z = \eta(x, y, t)$$

and the velocity there as

$$\vec{v} = (0, 0, \frac{\partial \eta}{\partial t})$$

and for a particle within the fluid the velocity is given by $\vec{u} = (u, v, w)$. We assume that the fluid particles do not cross the free surface hence

$$\vec{v}.\vec{n} = \vec{u}.\vec{n}$$

where $\vec{n} = (-\frac{\partial \nu}{\partial x}, -\frac{\partial \nu}{\partial y}, 1)$ is the unit normal drawn outwards at the free surface. Equating terms in the dot product above yields

$$\frac{\partial \nu}{\partial t} = -u\frac{\partial \nu}{\partial x} - v\frac{\partial \nu}{\partial y} + w$$

Since the free surface is at $z = H + h$ then we have $\eta(x,y,t) = H(x,y) + h(x,y,t)$. Using this in the above equation gives us the boundary condition at the surface as

$$\frac{\partial h}{\partial t} + \hat{u}\frac{\partial}{\partial x}(H+h) + \hat{v}\frac{\partial}{\partial y}(H+h) - \hat{w} = 0$$

where the "hat" on the velocity components indicates that they are evaluated at the free surface. In a similar manner, since fluid cannot penetrate the impermeable bottom $\Omega(z = -H)$, we obtain

$$\breve{u}\frac{\partial H}{\partial x} + \breve{v}\frac{\partial H}{\partial y} - \breve{w} = 0$$

where the breve is used to indicate the velocities are those at the bottom. We can apply the "no-slip" condition so that

$$\breve{u} = \breve{v} = \breve{w} = 0$$

3.0.1 Time-step limitations on the HPEs

The HPEs have time-step limitations due to existence of fast external gravity and Rossby modes. External waves as mentioned previously have propagation speeds as high as $200ms^{-1}$. This speed, c is obtained from the relation $c = \sqrt{gH}$, where g is the gravitational acceleration and H is the height of the water column.

3.0.2 External gravity waves

We have have already seen that acoustic waves if permitted can limit the time-step of an explicit large scale model to only the order of seconds. The HPEs are free of these waves since we already filtered the initial equations of these very fast speed modes. External gravity waves are the next fast modes after sound waves. We analyze these motions by depth-integrating the equations.
If the pressure is split into two parts

$$p = \int_z^\eta g\bar{\rho}dz + \int_z^\eta g(\rho - \bar{\rho})dz$$

then the external gradients of the first term on the right hand side will be uniform with depth and a function only of the free surface height:

$$\frac{1}{\bar{\rho}}\nabla_h \int_z^\eta g\bar{\rho}dz = g\nabla_h\eta$$

Using this in the depth averaged momentum equations (14) and the free surface equations we summarize

$$\frac{\partial}{\partial t}\int_{\Omega}\vec{v}_h d\Omega + g\nabla_h\eta = ...$$
$$\frac{\partial}{\partial t}\eta + \nabla.H\int_{\Omega}\vec{v}_h d\Omega = ...$$

Combining the two summary representations above we get

$$\frac{\partial^2}{\partial t^2}\eta - \nabla_h.gH\nabla_h\eta = ...$$

which is a representation of waves whose phase speed is given as $c_w = \sqrt{gH}$. For instance if $H = 4000m$ then $c_w = 200ms^{-1}$ which is very fast.
For resolutions of 10km and 100 km such an explicit time-step would be limited to an order of 1 minute and 8 minutes respectively. We can avoid these time limitations by filtering HPEs to remove the external waves. This is accomplished by use of three conventional methods namely;

i. Rigid-lid approximation

ii. the split-explicit method and

iii. the implicit method

3.0.3 Rigid-lid approximation

In the hydrostatic primitive equations, the total height of the water column is given as $h(x,y,t) = H(x,y) + \eta(x,y,t)$ where $z = \eta(x,y,t)$ is the surface elevation and $z = -H(x,y)$ is the length of the water column beneath a fixed level $z = 0$. In rigid-lid approximation we first assume that the free surface is at $z = 0$ and non-varying such that

$$D_t\eta = 0$$

As a result, equation (20) is modified into

$$\nabla.\int_{-H}^{0}\vec{v}_h dz = 0$$

The second step is to work on the pressure equation. We partition the pressure into two parts, one associated with the rigid lid denoted by p_s and an hydrostatic part p_h so that

$$p = p_s + p_h$$

The surface pressure, p_s is the pressure exerted by the rigid lid on the level surface $z = 0$ while the hydrostatic pressure is obtained by vertically integrating the hydrostatic equation from $z = 0$ to an arbitrary depth z and applying the boundary condition $p_h(0) = 0$;

$$p_h = \int_z^0 \frac{g\rho}{\bar{\rho}} dz$$

This further modifies the modifies the momentum equations to new form

$$\partial_t \vec{v}_h + \frac{1}{\bar{\rho}} \nabla_h p_s = \vec{G}_h$$

where $\vec{G}_h$ contains all the other missing terms including the lateral gradient of hydrostatic pressure. Discretization of this equation in time yields

$$\vec{v}_h^{n+1} + \frac{\Delta t}{\bar{\rho}} \nabla_h p_s = \vec{v}_h^n + \Delta t \vec{G}_h$$

Using this equation in the depth-integrated continuity equation gives

$$\frac{\Delta t}{\bar{\rho}} \nabla_h . H \nabla_h p_s = \nabla . \int_{-H}^0 (\vec{v}_h^n + \Delta t \vec{G}_h) dz$$

This form of approximation requires that we find $\vec{G}_h$ and then solve the elliptic equations to obtain the surface pressure. This is known as the **pressure method** and ensures non-divergence of the depth-integrated flows.
To solve the 2-D elliptic equations we require to specify the stream functions at the coasts (i.e. at $H = 0$) so as to be able to obtain the boundary conditions. The stream function was first used by Bryan and Cox in their first ocean model and clarifies that the elliptic equation need not be solved accurately.

3.0.4 Implicit free surface

The method is applied in time treatment of the free surface equation. It is a very stable method and does not limit the time step. For all types of oceanic flows, the free surface elevations are very small as compared to the nominal depth of the ocean $|\eta| << H$. This fact gives us a justification for linearizing the free surface equation (20) for the purposes of applying the implicit method (the implicit method is only suitable for linear terms). The equation for pressure (15) can be split into three integrals and written as

$$\begin{aligned} p = \int_z^\eta g\rho dz = \int_0^\eta g\bar{\rho} dz + \int_0^\eta g(\rho - \bar{\rho}) dz + \int_z^0 g\rho dz \\ \approx g\bar{\rho}\,\eta + \int_z^0 g\rho dz \end{aligned}$$

We next seek to linearize the free surface equation by making the assumption that $(\rho(\eta) - \bar{\rho}) << \bar{\rho}$ so that the approximate above becomes

$$p = g\bar{\rho}\eta + \int_z^0 g\rho dz$$

The next thing we do is to discretize the free-surface equation using the implicit backward method

$$\vec{v}_h^{n+1} + \Delta t g \nabla \eta^{n+1} = \vec{v}_h^n + \Delta t \vec{G}_h \tag{21}$$

$$\eta^{n+1} + \Delta t \nabla . \int_{-H}^0 \vec{v}_h^{n+1} d\nabla z = \eta^n + \Delta t (P - E) \tag{22}$$

Using equation (21) in Eq (22) to eliminate $\vec{v}_h^{n+1}$ we get

$$\eta^{n+1} + \Delta t^2 \nabla . gH \nabla \eta^{n+1} = \eta^n + \Delta t (P - E) - \Delta t \nabla . \int_{-H}^0 (\vec{v}_h^n + \Delta t \vec{G}_h) dz \tag{23}$$

an elliptic equation which we need to solve for η^{n+1} at each level in the model and then step forward the momentum equation.

3.0.5 Split-Explicit method

This one involves treating the depth-integrated equation differently from the rest of the equations in the system. The idea here is that we split this equation from the rest and integrate it using a shorter time-step. This is applied on this single equation because it is the equation that causes time-step limitations due to external gravity waves. First we find an approximate of the barotropic momentum equations

$$\partial_t \int_\Omega \vec{v}_h d\Omega + g \nabla \eta = \int_\Omega \vec{G}_h d\Omega \tag{24}$$

where $\int_\Omega \vec{G}_h d\Omega$ is the depth average of all the terms of the momentum equation. Next we integrate this Eq (24) with the free-surface equation forward using a short time step, $\frac{\Delta t}{M}$, with Δt being the regular time step for the entire full model. This is done using the forward-backward method outlined below

$$\eta^{\frac{n+(m+1)}{M}} = \eta^{\frac{n+m}{M}} + \frac{\Delta t}{M} \nabla . (H + \eta^{\frac{n+m}{M}}) \vec{v}_h^{\frac{n+m}{M}}$$

$$\vec{v}_h^{\frac{n+(m+1)}{M}} = \vec{v}_h^{\frac{n+m}{M}} + \frac{\Delta t}{M} (g \nabla \eta^{\frac{n+(m+1)}{M}} + < \vec{G}_h >)$$

These equations are then stepped forward M times to give the approximation for η^{n+1}.

3.0.6 Accelerating to equilibrium

Several manipulations are made on the equations to attain a fast convergence to equilibrium. A typical physical general circulation model would require roughly 7×10^{11} operations with 4050 grids to perform a complete computational model. This means that spinning up an ocean-climate model to equilibrium would take at least 1000 years. Thanks to Bryan for coming up with acceleration mechanism to help mathematicians realize accurate ocean models within a sensible time duration. Bryan, 1984, analyzed the method of accelerating ocean-climate models to converge fast to equilibrium. Accelerating the approach to equilibrium reduces the time needed to carry out computations by a large extend and eliminates the difficulty of the process. The consequences of the accelerating approach has been investigated extensively by Danabasoglu, McWilliams and Large J. Clim (1996) who gave support to the approach. In the following subsections, we will derive the dispersion relations for internal gravity waves then finally analyze the distortion.

3.0.7 Vertical modes

The linearized equations of motion are

$$\partial_t \vec{v}_h + f\hat{k} \wedge \vec{v}_h + \frac{1}{\rho}\nabla_h p = 0 \tag{25}$$

$$-b + \frac{1}{\rho}\partial_z p = 0 \tag{26}$$

$$\nabla_h . \vec{v}_h + \partial_z w = 0 \tag{27}$$

$$\partial_t b + wN^2 = 0 \tag{28}$$

where $b = -\frac{g\rho}{\bar{\rho}}$ is the buoyancy variable $N^2 = \partial_z b_0(z)$ is the background stratification for buoyancy. These equations are used for analysis of wave motions. To avoid the 3-D nature of these equations, we need to describe the vertical structure in terms of modes. To do this we use the Fourier modes and assume that the background stratification, N^2 is a constant. Every field can be described as a set of time and space dependent coefficients multiplying a vertical structure.

$$(\vec{v}_h, w, p, b) = \sum_m (\vec{v}_m, w_m, p_m, b_m) e^{imz}$$

This way we replace the vertical derivatives with im where $m = \frac{2\pi}{h_m}$ is the vertical wave number. Equations (26), (27) and (28) becomes respectively

$$b_m = imp_m$$
$$imw_m = -\nabla_h . \vec{v}_m$$
$$\partial_t b_m = N^2 w_m$$

These three are then combined together to give

$$m^2\partial_t\frac{p_m}{\bar{\rho}}+N^2\nabla_h v_m=0$$

and the four equations of motion (25) - (28) then reduces to

$$\partial_t\vec{v}_h+f\hat{k}\wedge\vec{v}_h+\frac{1}{\rho}\nabla_h p=0 \tag{29}$$

$$\partial_t\frac{p_m}{\bar{\rho}}+\frac{N^2}{m^2}\nabla_h v_m=0 \tag{30}$$

where $\frac{N}{m}$ is the gravity wave speed. These two are the equations that govern every vertical mode. They both take the form of shallow water equations. To obtain the dispersion relation for internal waves we assume another form for the vertical modes given by $e^{i(kx+ly-wt)}$ for each vertical mode. Working with this yields a dispersion relation of the form

$$\omega=f^2+(\frac{N}{m})^2(k^2+l^2)$$

Note that the background stratification N^2 can also be allowed to vary vertically as used bt Bryan, 1984. In this work we choose $N^2=$ constant to avoid complications since the results obtained in both choices have just a slight difference.

3.0.8 Slowing down inertia-gravity waves

To accelerate the motion we use shorter time steps in the momentum equation than in any other of the equations.

$$\Delta t_{\vec{v}}=\frac{1}{\alpha}\Delta t$$

where $\Delta t_{\vec{v}}$ is the horizontal time step, Δt the regular time step used in the full model and α is the distortion factor. This scales all the terms in the equation of momentum by α so that the new system becomes

$$\partial_t\vec{v}_h+\frac{1}{\alpha}(f\hat{k}\wedge\vec{v}_h+\frac{1}{\rho}\nabla_h p)=0 \tag{31}$$

$$-b+\frac{1}{\rho}\partial_z p=0 \tag{32}$$

$$\nabla_h.\vec{v}_h+\partial_z w=0 \tag{33}$$

$$\partial_t b+wN^2=0 \tag{34}$$

Using this new form of equations with a new time step applied to the momentum equation we repeat the process used in the previous subsection to reduce equations (32), (33) and (34) into a common equation. For the three combined together we get

$$\partial_t\frac{p_m}{\bar{\rho}}+(\frac{N}{m})^2\nabla_h.\vec{v}_m=0$$

so that the resulting equations for each vertical mode are given by

$$\alpha\partial_t\vec{v}_h + f\hat{k}\wedge\vec{v}_h + \frac{1}{\rho}\nabla_h\frac{p_m}{\bar{\rho}} = 0 \tag{35}$$

$$\partial_t\frac{p_m}{\bar{\rho}} + (\frac{N}{m})^2\nabla_h.\vec{v}_m = 0 \tag{36}$$

The dispersion relation for internal waves is obtained by another form of vertical modes given by $e^{kx+ly-wt}$ for each vertical mode. The dispersion relation is:

$$\omega^2 = \frac{f^2}{\alpha^2} + \frac{N^2}{\alpha m^2}(k^2+l^2)$$

For long waves $(k^2+l^2) << \frac{N^2}{(fm)^2}$ where the frequencies approach the Coriolis frequency, the distorted frequency is lower than α and the gravity wave speed is $\sqrt{\alpha}$ slower. The application of smaller time-step in the momentum equation slows down the fast waves.

Distorted Rossby waves

Using shorter time-step in the momentum equation also affects the Rossby waves (Rossby waves are also distorted). The geostrophic balance remains unaffected by the distortion factor α since the Coriolis and pressure gradient terms are equally scaled by α:

$$f\hat{k}\wedge v_m = \frac{1}{\rho}\nabla_h p_m$$

so that the vorticity can be written as

$$\zeta_m = \frac{1}{\rho}\nabla_h^2\frac{p_m}{\bar{\rho}}$$

Using this we express the vorticity equation as

$$\alpha\partial_t\xi_m + f\nabla_h\vec{v}_m + \beta v_m = 0$$

and the potential vorticity equation is

$$\frac{\alpha}{f}\partial_t\nabla_h^2 p_m - f\frac{m^2}{N^2}\partial_t p_m + \frac{\beta}{f}\partial_x p_m = 0$$

The dispersion relation of Rossby waves is given by

$$\omega = \frac{-\beta k}{\alpha(k^2+l^2) + \frac{f^2m^2}{N^2}}$$

For long waves $(k^2+l^2) << \frac{1}{L_r^2}$ and the distortion becomes negligible. Distortion can affect the stability of the models at western boundaries since short waves are slowed by time-stepping. The shallow water equations are given by

$$\alpha\partial_t\vec{v}_h + f\hat{k}\wedge\vec{v}_h + \frac{1}{\rho}\nabla_h\frac{p_m}{\bar{\rho}} = 0 \tag{37}$$

$$\partial_t\frac{p_m}{\bar{\rho}} + (\frac{N}{m})^2\nabla_h.\vec{v}_m = 0 \tag{38}$$

Splitting the momentum equation (37) into x- and y- components we have

$$\alpha\partial_t u_m - \beta y v_m + \partial_x\frac{p_m}{\bar{\rho}} = 0 \tag{39}$$

$$\alpha\partial_t v_m + \beta y u_m + \partial_y\frac{p_m}{\bar{\rho}} = 0 \tag{40}$$

$$\partial_t\frac{p_m}{\bar{\rho}} + \frac{N^2}{m^2}\nabla\vec{v}_m = 0 \tag{41}$$

Equations (39), (40)and (41) are the linear shallow water equations on the β-plane. These equations can be combined into a single equation of the form

$$\partial_t[\alpha^2\partial_{tt} + (\beta y)^2 - \alpha\frac{N^2}{m^2}\nabla_h^2]m - \beta\frac{N^2}{m^2}\partial_x v_m = 0 \tag{42}$$

We applied a rescaling to the meridional coordinates so that the new coordinates are $y' = \sqrt{\beta}y(\frac{\alpha m^2}{N^2})^{\frac{1}{4}}$. This results to a weak modification of equatorially trapped waves. The distorted linear bouyancy is given by

$$\partial_t b + \frac{\omega N^2}{\mu(z)} = 0$$

where $\mu(z) = 1$ at the surface and less than 1 in the interior of the fluid. N^2 being a constant indicates that $\frac{N^2}{\mu(z)}$ is purely a function of z or simply a function of depth. Hence modal decomposition of $\frac{N^2}{\mu(z)}$ must reflect the approximate vertical structure and the Fourier decomposition fails to work.

The method we have used here aims at accelerating the approach to equilibrium. It modifies the time-scales of the system to allow longer effective time-steps. We have used different time-steps for the thermodynamic tracer equations and the momentum equations. The convergence of this approach is most meaningful if there exists a steady state solution. This equation, (42) is not easy to solve. We will not solve this equation in this work, it is left to be solved in a further study by applying an appropriate method. This is the equation we intend to solve using the Discontinuous Galerkin Finite Element Method as per the topic of this project. The Navier-Stokes equations are the governing equations to most fluid dynamic models. They are the basis equations for models

concerning flows through thin channels (pipes), flows around aircrafts and ships, etc. to mention but a few. These equations are usually complicated and difficult to work with. To simplify them we make an assumption that the vertical acceleration in a fluid flow is negligible compared to the horizontal acceleration. This assumption is obvious for most flows on the earth's surface. Applying this assumption to the N-S equations results in a hydrostatic pressure distribution and the shallow water equations which are easy to deal with instead of the complicated N-S equations. The derivation here is based on the work of **Young et al**. (1997), **Vreugdenhil** (1994) and **Schwanenberg** (2003)

3.1 SWE for a flow through a Channel

In this section we derive the shallow water equations in one-dimension beginning with Navier Stokes equations which are free of the effects of rotation of the earth. For a small scale flow such as flow in a river/channel, dam or a lake, we may ignore the effects of earth's rotation. This leaves us with less complicated equations which can be solved with much ease. In this chapter we derive the 1D SWE. We begin with the N-S equations then apply the Boussinesq and hydrostatic approximations to obtain the 3D SWEs. This is then followed by application of subsequent conditions and integrations to the 3D SWE to obtain the 2D depth-integrated SWEs from which we then derive the 1D SWE.

3.1.1 3D shallow water equations

For a liquid (water in this context), the mass density remains more or less constant during motion. In this case we say that the flow is incompressible and we can express the density as

$$\rho = \rho(t,x) = \rho_0, \qquad \text{(all through the domain of flow)}$$

for some $\rho_0 > 0$. In this case the equation of mass conservation is given by

$$\frac{\partial u}{\partial x} + \frac{\partial v}{\partial y} + \frac{\partial w}{\partial z} = 0$$

The nature of this equation is kinematic. However, some experiments show that there exist flows whose velocity satisfy the equation above but whose density is dependent on the variables t and x. The incompressible N-S equations are made up of equation of conservation of mass above together with the equations of conservation of momentum.

The Cartesian form of the N-S equations is

$$\frac{\partial u}{\partial x}+\frac{\partial v}{\partial y}+\frac{\partial w}{\partial z}=0 \tag{43}$$

$$\frac{\partial u}{\partial t}+\frac{\partial u^2}{\partial x}+\frac{\partial (uv)}{\partial y}+\frac{\partial (uw)}{\partial z}=-\frac{1}{\rho}\frac{\partial p}{\partial x}+\nu(\frac{\partial^2 u}{\partial x^2}+\frac{\partial^2 u}{\partial y^2}+\frac{\partial^2 u}{\partial z^2}) \tag{44}$$

$$\frac{\partial v}{\partial t}+\frac{\partial (vu)}{\partial x}+\frac{\partial v^2}{\partial y}+\frac{\partial (vw)}{\partial z}=-\frac{1}{\rho}\frac{\partial p}{\partial y}+\nu(\frac{\partial^2 v}{\partial x^2}+\frac{\partial^2 v}{\partial y^2}+\frac{\partial^2 v}{\partial z^2}) \tag{45}$$

$$\frac{\partial w}{\partial t}+\frac{\partial (wu)}{\partial x}+\frac{\partial (wv)}{\partial y}+\frac{\partial w^2}{\partial z}=-\frac{1}{\rho}\frac{\partial p}{\partial z}+\nu(\frac{\partial^2 w}{\partial x^2}+\frac{\partial^2 w}{\partial y^2}+\frac{\partial^2 w}{\partial z^2}) \tag{46}$$

where (u,v,w) are velocity components in the (x,y,z) directions and $\nu=\frac{\mu}{\rho}$ is the kinematic viscosity, μ in the expression of ν is a constant representing the dynamic viscosity of water. p is the pressure and ρ is the mass density of water.
Using vector notation, let us denote by v_j the velocity components, x_j the directional indices, g the gravitational acceleration and σ_{ij} the deformation stresses then the $N-S$ equations can be represented using this notation as

$$\partial_{x_j} v_j = 0 \tag{47}$$

$$\partial_t v_i + \partial_{x_j}(v_j v_i - \frac{1}{\rho}\sigma_{ij}) = g_i \tag{48}$$

where Eq (47) is the mass conservation equation and Eq (48) the equation of momentum conservation. The index notation $i,j\in\{x,y,z\}$ represent the spatial directions and the partial derivatives are represented as $\partial_{x_j}=\frac{\partial}{\partial x_j}$. The stresses of deformation are in the form

$$\sigma_{ij}=-p\delta_{ij}+\mu(\partial_{x_j}v_i+\partial_{x_i}v_j)$$

where δ_{ij} is the Kronecker delta defined by

$$\delta_{ij}=\begin{cases}1, & \text{if } i=j\\ 0, & \text{if } i\neq j\end{cases}$$

In this conversion and in the entire work we assume that $g_x=g_y=0$ and $g_z=-g$
The depth of the fluid is given by $H(x,y,z)$ is a variable. The variation is caused by movements of water on the free water surface and changes in the level of the floor of the channel. At the free surface $z=\eta(x,y,t)$ but at the bottom face of the water layer, since we assume that the floor is not flat, the height there is depended on x and y but fixed in time, i.e. $z=-h(x,y)$. By fixing a reference level within the water layer at $z=0$ then the total depth will be given by

$$H(x,y,t)=h(x,y)+\eta(x,y,t) \tag{49}$$

The fluid depth and velocity are variables for which we seek solutions. The vertical acceleration is assumed to be negligible from the definition of shallow water flows. Thus in the z-momentum equation (46) we have that $|\frac{Dw}{Dt}| \ll |g + \frac{1}{\rho}\frac{\partial p}{\partial z}|$ and $|\nu\nabla^2 w| \ll |g + \frac{1}{\rho}\frac{\partial p}{\partial z}|$ where $\frac{Dw}{Dt}$ is the three dimensional material derivative given by $\frac{Dw}{Dt} = \frac{\partial}{\partial t} + u\frac{\partial}{\partial x} + v\frac{\partial}{\partial y} + w\frac{\partial}{\partial z}$ and $\nabla^2 = \frac{\partial^2}{\partial x^2} + \frac{\partial^2}{\partial y^2} + \frac{\partial^2}{\partial z^2}$ Thus the z-momentum equation can be approximately given by

$$\frac{1}{\rho}\frac{\partial p}{\partial x} = -g \tag{50}$$

which is the hydrostatic pressure distribution equation. Integrating this equation vertically and assuming that the atmospheric pressure is constant yields

$$p = \rho g(\eta - z) \tag{51}$$

Using equation (51) in equations (44) and (45) to substitute the pressure yields

$$\frac{\partial u}{\partial t} + \frac{\partial u^2}{\partial x} + \frac{\partial (uv)}{\partial y} + \frac{\partial (uw)}{\partial z} = -g\frac{\partial \eta}{\partial x} + \nu(\frac{\partial^2 u}{\partial x^2} + \frac{\partial^2 u}{\partial y^2} + \frac{\partial^2 u}{\partial z^2}) \tag{52}$$

$$\frac{\partial v}{\partial t} + \frac{\partial (vu)}{\partial x} + \frac{\partial v^2}{\partial y} + \frac{\partial (vw)}{\partial z} = -g\frac{\partial \eta}{\partial y} + \nu(\frac{\partial^2 v}{\partial x^2} + \frac{\partial^2 v}{\partial y^2} + \frac{\partial^2 v}{\partial z^2}) \tag{53}$$

The three equations (43), (51) (52) and (53) are the 3D shallow water equations (or incompressible hydrostatic Navier-Stokes equations). The unknowns are the velocity components u, v, w and the surface elevation η
We can evaluate the vertical velocity of a fluid particle at the free surface and that of a fluid particle at the bottom. To evaluate these velocities, we assume that a fluid particle at the bottom or at the top retains its position respectively.

$$\text{At the surface: } w|_{z=\eta} = \frac{D\eta}{DT}|_{z=-h} = [\frac{\partial \eta}{\partial t} + u\frac{\partial \eta}{\partial x} + v\frac{\partial \eta}{\partial y}]_{z=\eta} \tag{54}$$

$$\text{and at the bottom: } w|_{z=-h} = -\frac{Dh}{Dt}|_{z=-h} = -[u\frac{\partial h}{\partial x} + \frac{\partial h}{\partial y}]_{z=-h} \tag{55}$$

Equations (54) and (55) are known as the kinetic boundary conditions for the 3D SWEs.

3.1.2 2D shallow water equations

They are obtained by further integration of the 3D SWEs vertically over the water depth. Starting with the continuity equation (43) and integrating over the interval $z = [-h, \eta]$;

$$\int_{-h}^{\eta} \frac{\partial}{\partial x} u dz + \int_{-h}^{\eta} \frac{\partial}{\partial y} v dz + \int_{-h}^{\eta} \frac{\partial}{\partial z} w dz = 0$$

We recall the Leibniz's theorem which asserts that;

$$\frac{\partial}{\partial\beta}\int_{\lambda_1(\beta)}^{\lambda_2(\beta)} f(\lambda,\beta)d\lambda = \int_{\lambda_1(\beta)}^{\lambda_2(\beta)} \frac{\partial}{\partial\beta} f d\lambda + f(\lambda_2,\beta)\frac{\partial\lambda_2}{\partial\beta} + f(\lambda_1,\beta)\frac{\partial\lambda_1}{\partial\beta}$$

Applying this we can integrate the above terms of the integrals of the continuity equation to obtain

$$\frac{\partial}{\partial x}\int_{-h}^{\eta} u dz - u|_{z=\eta}\frac{\partial\eta}{\partial x} - u|_{z=-h}\frac{\partial h}{\partial x} + \frac{\partial}{\partial y}\int_{-h}^{\eta} v dz - v|_{z=-h}\frac{\partial\eta}{\partial y} - v|_{z=-h}\frac{\partial h}{\partial y} + w|_{z=\eta} - w|_{z=-h} = 0$$

The depth averaged velocity terms are given as

$$\bar{u} = \frac{1}{H}\int_{-h}^{\eta} u dz \qquad \text{and} \qquad \bar{v}\int_{-h}^{\eta} v dz \tag{56}$$

We use these definitions to eliminate the integrals from the equation above to obtain

$$\frac{\partial(\bar{u}H)}{\partial x} - u|_{z=\eta}\frac{\partial\eta}{\partial x} - u|_{z=-h}\frac{\partial h}{\partial x} + \frac{\partial(\bar{v}H)}{\partial y} - v|_{z=-h}\frac{\partial\eta}{\partial y} - v|_{z=-h}\frac{\partial h}{\partial y} + w|_{z=\eta} - w|_{z=-h} = 0$$

To obtain the boundary conditions at the bottom and on the surface, we substitute the kinetic boundary conditions (54) and (55) in this equation to get

$$\frac{\partial\eta}{\partial t} + \frac{\partial}{\partial x}(\bar{u}H) + \frac{\partial}{\partial y}(\bar{v}H) = 0 \tag{57}$$

From the definition of the height of the water column in Eq (49), $\eta = H - h(x,y)$. This guides us to seeing that the continuity equation in two-dimensions can be written as

$$\frac{\partial H}{\partial t} + \frac{\partial}{\partial x}(\bar{u}H) + \frac{\partial}{\partial y}(\bar{v}H) = 0 \tag{58}$$

expressed in the form of derivatives of the depth averaged velocities and a time derivative of the height of the column.

A similar treatment is carried out on the momentum equations i.e. depth-integrating the individual terms. For the x-momentum equation, Eq (52), applying the Leibniz's formula

to integrate each term;

$$\int_{-h}^{\eta} \frac{\partial}{\partial t} u dz = \frac{\partial}{\partial t} \int_{-h}^{\eta} u dz - u|_{z=\eta} \cdot \frac{\partial \eta}{\partial t} \tag{59}$$

$$\int_{-h}^{\eta} \frac{\partial}{\partial x} u^2 dz = \frac{\partial}{\partial x} \int_{-h}^{\eta} u^2 dz - u^2|_{z=\eta} \cdot \frac{\partial \eta}{\partial x} - u^2|_{z=-h} \cdot \frac{\partial h}{\partial x} \tag{60}$$

$$\int_{-h}^{\eta} \frac{\partial}{\partial y} (uv) dz = \frac{\partial}{\partial y} \int_{-h}^{\eta} (uv) dz - (uv)|_{z=\eta} \cdot \frac{\partial \eta}{\partial y} - (uv)|_{z=-h} \cdot \frac{\partial h}{\partial y} \tag{61}$$

$$\int_{-h}^{\eta} \frac{\partial}{\partial z} (uw) dz = (uw)|_{z=\eta} - (uw)|_{z=-h} \tag{62}$$

$$\int_{-h}^{\eta} g \frac{\partial}{\partial x} \eta dz = g \frac{\partial}{\partial x} \eta (\eta + h) = gH \frac{\partial}{\partial x} (H - h) \tag{63}$$

Depth-integrating the last term on the right hand side of equation (52) we obtain the depth-integrated friction denoted by S_{f_x} and given by

$$S_{f_x} = \int_{-h}^{\eta} \nu \left(\frac{\partial^2 u}{\partial x^2} + \frac{\partial^2 u}{\partial y^2} + \frac{\partial^2 u}{\partial z^2} \right) dz$$

Since the velocity variation vertically is negligible we can take out the integrands involving velocities from equations (59), (60) and (61) since the values of these terms turn out to be negligible. Also let us take equality of the depth-integrated velocities to the horizontal velocities,i.e. $\bar{u} = u$ and $\bar{v} = v$. Then applying the kinetic boundary conditions (54) and (55) to the depth-integrated x-momentum equation yields

$$\frac{\partial}{\partial t} (uH) + \frac{\partial}{\partial x} (u^2 H) + \frac{\partial}{\partial y} (uvH) = gH \frac{\partial}{\partial x} (h - H) + S_{f_x} \tag{64}$$

where $S_{f_x} = \int_{-h}^{\eta} \nu \left(\frac{\partial^2 u}{\partial x^2} + \frac{\partial^2 u}{\partial y^2} + \frac{\partial^2 u}{\partial z^2} \right) dz$ is the depth-integrated term of the x-component. Carrying out a similar operation on Eq (53) we obtain the depth-integrated y-momentum equation which takes the form

$$\frac{\partial}{\partial t} (vH) + \frac{\partial}{\partial x} (vH) + \frac{\partial}{\partial y} (v^2 H) = gH \frac{\partial}{\partial y} (h - H) + S_{f_y} \tag{65}$$

where S_{f_y} is the depth-integrated friction term.
Equations (58), (64) and (65) are the two dimensional shallow water equations.

$$\frac{\partial H}{\partial t} + \frac{\partial}{\partial x} (\bar{u} H) + \frac{\partial}{\partial y} (\bar{v} H) = 0 \tag{66}$$

$$\frac{\partial}{\partial t} (uH) + \frac{\partial}{\partial x} (u^2 H) + \frac{\partial}{\partial y} (uvH) = gH \frac{\partial}{\partial x} (h - H) + S_{f_x} \tag{67}$$

$$\frac{\partial}{\partial t} (vH) + \frac{\partial}{\partial x} (vH) + \frac{\partial}{\partial y} (v^2 H) = gH \frac{\partial}{\partial y} (h - H) + S_{f_y} \tag{68}$$

This is the system of shallow water equations representing mass and momentum conservation. We can write them in the differential conservative law form as

$$\frac{\partial \vec{u}}{\partial t} + \nabla . f(\vec{u}) = S(\vec{u}) \tag{69}$$

where $\nabla f = \partial_x f_x + \partial_y f_y, \vec{u}$ is a vector containing the unknown variables, $\vec{f} = (\vec{f_x}, \vec{f_y})$ is a flux vector and $S(\vec{u})$ is the vector containing the source terms. Here

$$\vec{u} = \begin{bmatrix} H \\ uH \\ vH \end{bmatrix} \qquad f_x(\vec{u}) = \begin{bmatrix} uH \\ u^2H \\ uvH \end{bmatrix}$$

$$f_y(\vec{u}) = \begin{bmatrix} vH \\ uvH \\ v^2H \end{bmatrix} \qquad \text{and} \qquad S(\vec{u}) = \begin{bmatrix} 0 \\ -gH\frac{\partial \eta}{\partial x} + S_{f_x} \\ -gH\frac{\partial \eta}{\partial y} + S_{f_y} \end{bmatrix}$$

or

$$\vec{u} = \begin{bmatrix} H \\ uH \\ vH \end{bmatrix} \qquad f_x(\vec{u}) = \begin{bmatrix} uH \\ u^2H + \frac{1}{2}gH^2 \\ uvH \end{bmatrix}$$

$$f_y(\vec{u}) = \begin{bmatrix} vH \\ uvH \\ v^2H + \frac{1}{2}gH^2 \end{bmatrix} \qquad \text{and} \qquad S(\vec{u}) = \begin{bmatrix} 0 \\ gH\frac{\partial h}{\partial x} + S_{f_x} \\ gH\frac{\partial h}{\partial y} + S_{f_y} \end{bmatrix}$$

3.1.3 One-dimensional SWE

For flows in channels and rivers we neglect the acceleration in the y-direction. This further reduces the 2D SWE into a one-dimensional equation. The equations are simplified by looking at the cross-section instead of the total water depth.
Consider an incompressible 1D flow. Let us take an infinitesimal fluid volume in the flow of a cross-sectional areas $A(x)$ on one face and $A(x+\triangle x)$ on the other face. Also let the pressure acting on the face of cross section $A(x)$ be $p(x)$ and that acting on the second face be $p(x+\triangle x)$. Then the Navier Stokes equations for this infinitesimal control volume without viscous stress terms are given by

$$\partial_t(A \triangle x) - (Au)(x) + (Au)(x+\triangle x) = 0 \tag{70}$$

$$\partial_t(Au \triangle x) - (Au^2)(x) + (Au^2)(x+ \triangle x)$$

$$= \frac{1}{\rho}[(Ap)(x) - (Ap)(x+ \triangle x)] + \frac{1}{\rho}p[A(x+ \triangle x) - A(x)] \tag{71}$$

where $\triangle x$ is the length of the selected control volume and p is the normal pressure acting on the infinitesimal control volume. Dividing equations (69) and (70) by $\triangle x$ and taking the limit as $\triangle x \longrightarrow 0$ we obtain the differential equations given below

$$\partial_t A + \partial_x(Au) = 0 \tag{72}$$

$$\partial_t(Au) + \partial_x(Au^2) = -\frac{1}{\rho}A\partial_x p \tag{73}$$

Applying the hydrostatic pressure condition since the flow here is a shallow water flow, the equations are further modified into

$$\partial_t A + \partial_x(Au) = 0 \tag{74}$$

$$\partial_t(Au) + \partial_x(Au^2) = gA\partial_x(h-H) \tag{75}$$

These are the one-dimensional shallow water equations. To obtain the (quasi-) conservation law form of these equations, we further differentiate the R.H.S term on equation (75) to get

$$\partial_t A + \partial_x(Au) = 0 \tag{76}$$

$$\partial_t(Au) + \partial_x(Au^2 + gAH) = gA\partial_x h - gH\partial_x A \tag{77}$$

We still need to modify the equations further to obtain the equations in a completely conservation law form. We will do this by making the assumption that the channel is of a constant width W, so that $A = HW$. Inserting this value of A in Eq (74) and (75) we obtain

$$\partial_t H + \partial_x(uH) = 0 \tag{78}$$

$$\partial_t(uH) + \partial_x(u^2H) = gH\partial_x(h-H) \tag{79}$$

Let $q = uH$ be the discharge and η the surface elevation then the equations further reduces to the form

$$\partial_t H + \partial_x(q) = 0 \tag{80}$$

$$\partial_t(q) + \partial_x(uq) = -gH\partial_x\eta \tag{81}$$

The term on the right hand side of (81) represents the surface slope and it brings about variations in the discharge.
If the conservative form of the equations are required to include the momentum flux,

then we represent the bottom slope as the source term so as to facilitate this. The surface becomes no longer the source term as in the above equations and (80) is modified and we have the new form of the equations as

$$\partial_t H + \partial_x(q) = 0 \tag{82}$$

$$\partial_t(q) + \partial_x(\frac{q^2}{H} + \frac{1}{2}gH^2) = gH\partial_x h \tag{83}$$

which can be written in conservative law form as

$$\partial_t \mathbf{u} + \partial_x f(\mathbf{u}) = s(\mathbf{u}) \tag{84}$$

where

$$\mathbf{u} = \begin{bmatrix} H \\ q \end{bmatrix}, \qquad f(\mathbf{u}) = \begin{bmatrix} q \\ \frac{q^2}{H} + \frac{1}{2}gH^2 \end{bmatrix} \qquad \text{and } s(\mathbf{u}) = \begin{bmatrix} 0 \\ -gH\partial_x h \end{bmatrix} \tag{85}$$

This equation represents a one-dimensional SWE where $f(\mathbf{u}) = \begin{bmatrix} q \\ \frac{q^2}{H} + \frac{1}{2}gH^2 \end{bmatrix}$ is the fluid flux and $s(\mathbf{u}) = \begin{bmatrix} 0 \\ -gH\partial_x h \end{bmatrix}$ is the source term. We will solve this equation using the Discontinuous Galerkin finite element (DG) discussed in the next chapter.

4 Finite Element Methods for PDEs

4.1 Introduction: Partial Differential Equations (PDEs)

PDEs are Mathematical expressions describing a relation between dependent variable $u(\mathbf{x})$ and independent variables $\mathbf{x}$ through multiplications and partial derivatives. The **order** of a differential equation is defined as the order of the highest derivative of $u(\mathbf{x})$ that appears in the equation. A general second order PDE with constant coefficients takes the form

$$Au_{xx}(x,y) + 2Bu_{xy}(x,y) + cu_{yy}(x,y) + Du_x(x,y) + Eu_y(x,y) + Fu(x,y) = G$$

The PDE is said to be homogeneous if $G = 0$ and non-homogeneous if otherwise. These differential equations can either be classified as **Elliptic, Parabolic** or **hyperbolic** depending on the value of the discriminant $d = AC - B^2$. If $d > 0$ we say that the PDE is **Elliptic**, if $d = 0$ we classify the PDE as **Parabolic** and if $d < 0$ the PDE is said to be **Hyperbolic**. Examples:

i **Elliptic**: The Laplacian equation, $\frac{d^2u}{dx^2} + \frac{d^2u}{dy^2} = 0$

ii **Parabolic**: Heat equation, $\frac{du}{dt} - \frac{d^2u}{dx^2} = 0$

iii **Hyperbolic**: Wave equation, $\frac{d^2u}{dt^2} - \frac{d^2u}{dx^2} = 0$

Initial conditions and/or boundary requirements are given together with these expressions. Depending on the conditions given, we come up with three types of problems namely; **Initial Value Problems** (IVP), **Boundary Value Problems** (BVP) and **Initial Boundary Value Problems**(IBVP).

i. **Initial value problem**
An IVP is a problem in which the value of the dependent variable and its derivative is specified at the initial point $t = 0$ or at some value of the independent variables in the equation. Example: Below shows an IVP of the wave equation

$$\begin{cases} \frac{d^2u}{dt^2} - \frac{d^2u}{dx^2} = 0 & -\infty < x < \infty \qquad t > 0 \\ u(x,0) = f(x), \qquad u_t(x,0) = g(x), & -\infty < x < \infty \end{cases}$$

ii. **Boundary value problem**
In this type of a problem, the value of the dependent variable and possibly its derivatives are specified at the extreme values of the independent variable. For example: The 1D stationary heat equation

$$\begin{cases} -[a(x)u^{'}(x)]^{'} = f(x), & 0 < x < 1 \\ u(0) = u_0, \qquad u(1) = u_1, \text{ where } u_0, u_1 \in R \end{cases}$$

There are three types of boundary conditions namely;

1. *Dirichlet boundary condition*: The value of the depended variable u is specified at the boundary.

$$u(x,t) = f(x), \qquad \text{for } \mathbf{x} = (x_1, x_2, \ldots, x_n) \in R^n, t > 0$$

2. *Neumann boundary conditions*: In this type of BC the derivative of the solution at the direction of the outward normal vector is provided For the heat equation for instance;

$$\begin{cases} \frac{du}{dt} - \frac{d^2u}{dx^2} = 0 \\ \frac{\partial u}{\partial \mathbf{n}} = \mathbf{n}.\text{grad}(u) = n.\nabla u = f(x), \qquad \mathbf{x} \in \partial\Omega \end{cases}$$

where $\mathbf{n} = \mathbf{n}(\mathbf{x})$ is an outward unit normal to $\partial\Omega$ at $\mathbf{x} \in \partial\Omega$

3. *Robin boundary conditions*: Also called Mixed boundary conditions. It is a combination of the Dirichlet and the Neumann boundary conditions.

iii. **Initial boundary value problem**
In this problem we have both the initial conditions and the boundary conditions given.

Solutions of PDEs can then use this information and give us predictions of the later states of this information. Mathematically, partial differential equations are equations which contains partial derivatives, three examples of PDEs have been used previously in examples. Here we introduce another PDE called the Poisson equation which is given by

$$\Delta u = \nabla^2 \frac{\partial^2 u}{\partial x^2} + \frac{\partial^2 u}{\partial y^2} = f \tag{86}$$

4.1.1 Methods of solving PDEs

There are several solution methods that can be used depending on the nature of the physical problem. These include the Finite difference method, finite element method and the finite volume method. The finite difference method is the most commonly used. It

uses discrete approximations from grid information to replace the partials. For example, in the Poisson equation we have the following operator acting on u

$$L = \nabla^2 = \frac{\partial^2}{\partial x^2} + \frac{\partial^2}{\partial y^2}$$

Then the equation can be written as $Lu = f$. Finite Difference methods are based on approximating this operator by a discrete operator. Unlike the FEM, the FDM is not very accurate if the geometry of the domain is complex. This difference between these two methods comes in at the point of discretizing the PDE. Reed and Hill, (1971) came up with a modification of the finite element method namely the Discontinuous Galerkin finite element method. The need of this new method was to solve the neutron transport equation. Unlike the FEM, this method makes use of discontinuous approximating functions.

The finite element method is a very rigorous method for solving PDEs. PDEs are Mathematical expressions describing a relation between dependent and independent variables through multiplications and partial derivatives. Initial conditions and boundary requirements are given together with these expressions. Solutions of PDEs can then use this information and give us predictions of the later states of this information. Mathematically, partial differential equations are equations which contains partial derivatives, examples of PDEs are the wave equations, heat equations, Laplace equations, Poisson equation etc. The Poisson equation for example is given by

$$\Delta u = \nabla^2 \frac{\partial^2 u}{\partial x^2} + \frac{\partial^2 u}{\partial y^2} = f \tag{87}$$

We will use this example in the practical examples and when introducing the finite element method (FEM). In this equation u depends symmetrically on x and y. So, if we choose a symmetric Ω, the solution will be symmetric.
In solving this equation, we find the solution in the region Ωdefined by$\Omega = (-1,1)^2$.. These boundary conditions are fundamental for the formulation of the finite element mathod.

4.1.2 Finite element Method

The finite element method is mathematically very rigorous. It has much stronger mathematical foundation than many other methods i.e. it is mathematically more elaborate than many other methods, and particularly the finite difference method. FEM uses results from real and functional analysis. In the practical example in the end, we have included what we call the minimization principle. This is equivalent to the minimizing principle used when deriving the conjugate gradient method by minimizing the quadratic function. The answer to this minimization function is our solution. But there is another result, called

Weak formulation, which, when true, also makes the minimization formulation true. So we will start at the weak formulation and discuss the results we arrive at. FEM is a numerical method of solving PDEs, and to achieve this objective, it is a characteristic feature of the FE approach that the PDE in question is first reformulated into an equivalent form, and this form has a weak form.

4.1.3 Steps in the Finite Element Approach

The final formulation of the FE method is a linear system $Au = b$. These are the steps followed in the FE approach

i. Establish the strong formulation

ii. Obtain the weak formulation

iii. Choose approximations for the unknown functions, in this case u

iv. Choose the weight functions v

v. Solve the resulting linear system

4.1.4 Strong Formulation (Poisson Equation)

In this part we consider the Poisson equation chosen in the beginning. We want to solve this in the region $\Omega = (0,1)^2$ We intend to use only Homogeneous Dirichlet boundary conditions. This gives us

$$\Delta u = \frac{\partial^2 u}{\partial x^2} + \frac{\partial^2 u}{\partial y^2} = f, \text{defined on} \Omega = (0,1)^2 \tag{88}$$

$$u(\partial\Omega) \qquad \partial\Omega = \{(x,y)|x = 0,1 \text{ or } y = 0,1\}. \tag{89}$$

This is called the *strong formulation* in Finite element, and says no more than the original PDE formulation.

4.1.5 Weak Formulation (Poisson's Equation)

The weak formulation is a re-formulation of the original PDE (strong form), and it is from this form that we establish the final FE approach. To establish the weak form of the PDE, we multiply equation (88) with an arbitrary function, so-called *weight-function* $v(x,y)$ to obtain

$$v\nabla^2 u = fv \tag{90}$$

Integrating this expression over Ω.

$$\int_\Omega v\nabla^2 u = \int_\Omega fv \tag{91}$$

$v(x,y)$ should be chosen in such a way that the manipulations it undergoes are meaningful. Let us define a space of functions and call it H^1

$$H^1(\Omega) = \{v : \Omega \longrightarrow R : \int_\Omega v^2, \int_\Omega v_x^2, \int_\Omega v_y^2 < +\infty\} \tag{92}$$

H^1 is a function space where all the functions are bounded [quadratic integrable]. We want our functions to be well-behaved, so that we can define operations on them within the rules of, say, integration. Let us now define a sub-space X of H^1 and let

$$X = \{v \in H^1(\Omega) : v|_{\partial\Omega} = 0 \tag{93}$$

Integrating further eguation (92). Let $u, v \in X$. We know from calculus that $\nabla(v\nabla u = \nabla v.\nabla u + v\nabla^2 u)$. We can write

$$\int_\Omega v\nabla^2 u = \int_\Omega \nabla v.\nabla u \tag{94}$$

Using Gauss's theorem on $\nabla(v\nabla u)$ we get

$$\int_\Omega (v\nabla u) = \int_{\partial\Omega} v \underbrace{v|_{\partial\Omega=0}}\nabla u.\hat{n}dS = 0 \tag{95}$$

In equation (95), we have transformed a surface integral to a line integral and dS refers to an infinitesimal line segment. We have not put dA on the surface integrals, therefore, Eq (94) reduces to

$$\int_\Omega v\nabla^2 u = -\int_\Omega \nabla v.\nabla u \tag{96}$$

and, so we get

$$-\int_\Omega \nabla v.\nabla u dA = \int_\Omega fv dA \tag{97}$$

Advantages of Weak Form Compared to Strong Form

Eq (97) is the final weak formulation. It is equivalent to the strong form posed previously. In the strong form, we have two separate partial derivatives of u, so the strong form requires that u be continuously differentiable until at least second partial derivatives. Our

new formulations has lowered this requirement to only first partial derivatives of u by transforming one of the partial derivatives onto the weight-function $v(x,y)$. This is the first big advantage of the weak formulation.
X is a subspace of H_1 because our weak form requires that the functions be in H^1. The strong form requires that u be 0 along the boundary, so X is the subspace of all functions which are zero on the boundary. Note that, Dirichlet are essential and reflected in X. This comes automatically when we use the weak form.

4.1.6 Approximating the Unknown u

In the FE method, the region is divided into smaller parts and the approximation is carried out over these smaller parts, and then based on these results, it is established for the entire region. The entire domain is split into smaller parts called *finite elements,* for which we are able to give an approximation for u, then we are able to approximate u for the whole geometry of any form. Hence we say that the approximation has been carried out "elementwise", hence the name.
The following diagrams shows one dimensional elements;

Figure 1. Linear 1-D element

Figure 2. Quadratic 1-D element

Figure 3. Cubic 1-D element

In 2-dimensions the elements are triangular and can be linear, quadratic or cubic as shown in the next figure. The domain is first discretized into nodes, and then well-defined triangulation is performed between the nodes. Elements may share nodes with some even having four or more nodes. The advantage of triangulation is that it can be used to approximate a huge range of geometries.

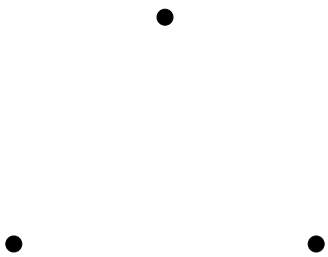

Figure 4. Nodes for a 2-D linear element

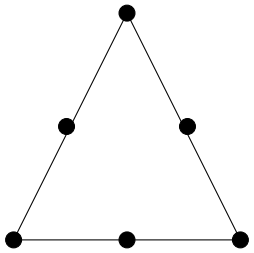

Figure 5. 2-D Quadratic element

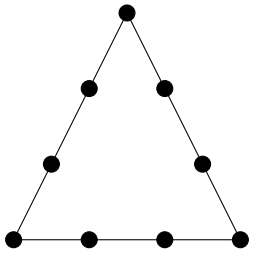

Figure 6. 2-D cubic element

4.1.7 Basis Functions

The discretization of the 2D-domain is made up of triangles and each triangle has three nodes. One node can be shared by several triangles whereby each triangle is an element. The final formulation will give us a linear system of equations with dimensions $N \times N$ where N is the number of nodes. This means that after solving the system, we will find the values of u at the nodes.

We need to define basis functions for the 2D-domain. We will have as many basis functions as we have nodes, i.e. each node has one basis function. We denote these basis functions (for node number i) as $\phi(x_j, y_j) = \delta_{ij}$. Each $\phi_i(x,y)$ is non-zero only in elements which share node i.

Going back to the weak form of our equation, Eq (97), let us look at the function $u(x,y)$ which is continuously differentiable. Note that all the functions ϕ_i are continuously differentiable.

In our problem, we are in search of a function $\hat{u}(x,y)$ which is piecewise linear on each element. The function we are looking for can be written as a linear combination of the basis functions as

$$\hat{u}(x,y) = \sum_{i=1}^{N} \hat{u}_i \phi_i(x,y) \tag{98}$$

and again

$$\hat{u}(x_j, y_j) = \sum_{i=1}^{N} \hat{u}_i \phi_i(x_j, y_j) = \hat{u}_j, \text{Nodal basis} \tag{99}$$

We can define other forms say l and a so as to express our problem in an easy form. Let us define these two forms as

$$a(u,v) \equiv \int_\Omega \nabla v.\nabla u \text{ and } l(v) \equiv \int_\Omega fv \tag{100}$$

Using integral rules we observe that a is a bilinear form and l is a linear form. Using Eq (100) and the weak form Eq (97), the weak form can be re-written as

$$a(u,v) = l(v), \qquad u,v \in X \tag{101}$$

also notice that $a(u,v) = a(v,u)$.
Note that the number N used in the summations above is the number of nodes, the boundary nodes included. We can at this stage express our approximation function $\hat{u}$ and our weight function v respectively as

$$\hat{u} = \sum_{i=1}^{N} \hat{u}_i \phi_i \tag{102}$$

$$v = \sum_{j=1}^{N} v_j \phi_j \tag{103}$$

Note that we are using v in terms of our basis functions. This is called the Galerkin method. Putting Eq (102) and (103) into the weak form, Eq (101) above we have

$$\begin{aligned} a(\sum_{j=1}^{N} v_j\phi_j, \sum_{i=1}^{N} \hat{u}_i) &= l(\sum_{j=1}^{N} v_j\phi_j) \\ &= a(v_1\phi_1, \sum_{j=2}^{N} v_j\phi_j, \sum_{i=1}^{N} \hat{u}_i\phi_i) \\ &= a(v_1\phi_1, \sum_{i=1}^{N} \hat{u}_i\phi_i) + a(\sum_{j=2}^{N} v_j\phi_j, \sum_{i=1}^{N} \hat{u}_i\phi_i) \\ &= \sum_{j=1}^{N} a(v_j\phi_j, \sum_{i=1}^{N} \hat{u}_i\phi_i) \\ &= \sum_{j=1}^{N}\sum_{i=1}^{N} a(v_j\phi_j, \hat{u}_i\phi_i) \\ &= \sum_{j=1}^{N} v_j \sum_{i=1}^{N} a(\phi_j,\phi_i)\hat{u}_i = \sum_{j=1}^{N} v_j l(\phi_j) \end{aligned} \tag{104}$$

The last expression can be written in compact form as

$$v^T A\hat{u} = v^T F \Longrightarrow A\hat{u} = F \tag{105}$$

Here,

$$v = [v_1, v_3, ..., v_N]^T \tag{106}$$

$$\hat{u} = [\hat{u}_1, \hat{u}_3, ..., \hat{u}_N] \tag{107}$$

and A and F are given by

$$A = \begin{bmatrix} a(\phi_1,\phi_2 & a(\phi_1,\phi_2) & \dots & a(\phi_1,\phi_N) \\ a(\phi_2,\phi_1) & a(\phi_2,\phi_2) & \dots & a(\phi_2,\phi_N) \\ \dots & \dots & \dots & \dots \\ a(\phi_N,\phi_1) & a(\phi_N,\phi_2) & \dots & a(\phi_N,\phi_N) \end{bmatrix} \text{ and } F = \begin{bmatrix} l(\phi_1 & l(\phi_2) & \cdots & l(\phi_N) \end{bmatrix}^T \tag{108}$$

Note that the system $A\hat{u} = F$ is not symmetric positive definite (SPD), a property that is a prerequisite for the conjugate gradient method. The reason for this is because we have not yet specified the boundary conditions. We have just set up the system for all nodes. We need to change this system so that $u = 0$ along the boundary. Remember that we had $u = 0$ in our strong form. We also have $f = 1$, so that there is no need to use quadrature or any other numerical technique to calculate the $l(\phi_i)$ integral, since this integral is easy to calculate.
If our node numbering is given as $1, 2, 3, ..., N$, we can easily change our linear system to an SPD by setting $\hat{u} = 0$ for all nodes i which are boundary nodes. If for instance the fourth node is a boundary node we remove the fourth column and the fourth row from the matrix A. After removing all the rows and columns corresponding to the boundary nodes, we will have the final SPD form of the linear system which can be solved by the several numerical methods.
Towards our practical implementation, it will be convenient to define a reference triangular element and define a $1-1$ mapping between a general physical element in the physical domain. All the integrals which make up A and F are performed in this reference element. This is just a convenient substitution.

4.1.8 Solving the Poisson Equation

As seen previously, the Poisson equation is given as $\Delta u = \nabla_2 u = f = 1$, defined on the region $\Omega =$ Let us denote the boundary by Γ

4.1.9 Minimization formulation

We seek to find $u \in V_D$ such that

$$u = \arg\min_{w \in VD} J(w) \tag{109}$$

$$J(w) = \frac{1}{2}\int_\Omega \nabla w.\nabla w dA - \int_\Omega f w dA \tag{110}$$

$$= \frac{1}{2}\int_\Omega \nabla w.\nabla w dA \tag{111}$$

$$V^D = \{v \in H^1(\Omega) | v|_\Gamma = 0\} \tag{112}$$

$$H_1(\Omega) = \{v : R \longrightarrow R | \int_\Omega v^2, \int_\Omega v_x^2, \int_\Omega v_y^2 < ++\infty\} \tag{113}$$

4.1.10 Weak formulation

Let $w = u + v \in V^D$.

$$\begin{aligned} J(w) = J(u+v) \\ &= \frac{1}{2}\int_\Omega \nabla(u+v).\nabla(u+v) dA \\ &= \frac{1}{2}\int_\Omega \nabla u.\nabla v dA + \int_\Omega \nabla u.\nabla v dA + \frac{1}{2}\int_\Omega \nabla v.\nabla v dA \end{aligned} \tag{114}$$

$$\begin{aligned} \delta J_v(U) = \int_\Omega \nabla u.\nabla v dA \\ &= \int_\Omega \nabla(v\nabla u) dA - \int_\Omega v\nabla^2 u dA \\ &= \int_\Gamma v\nabla u.\hat{n} dS - \int_\Omega v\nabla^2 u dA = 0 \end{aligned} \tag{115}$$

It follows from the above results that

$$J(w) \geq J(u) \qquad \forall w, u \in V^D, \qquad \text{Weak formulation} \tag{116}$$

4.1.11 Geometric representation

Let $\phi_i|_T = N_i$. This is the function ϕ_i restricted to one element. T stands for an element. We want to compute the integral over the element T

$$a(N_i, N_j) = \int_T \frac{\partial N_i}{\partial x}\frac{\partial N j}{\partial x} + \frac{\partial N_i}{\partial y}\frac{\partial N_j}{\partial y} dA \tag{117}$$

In terms of programming, it is easier to calculate the element integral (117) by the use of substitution. We define a linear and affine mapping between T and a reference element $\hat{T}$ for simplicity. Basis functions for $\hat{T}$ corresponding to the functions $N_1(x,y), N_2(x,y)$ and $N_3(x,y)$ are given by

$$\hat{N}(\xi,\eta) = 1-\xi-\eta$$

$$\hat{N}_2(\xi,\eta) = \xi$$

$$\hat{N}_3(\xi,\eta) = \eta \tag{118}$$

The relationship between the coordinates (x,y) and (ξ,η) is given by

$$x = x_1^T\hat{N}_1 + x_2^T\hat{N}_2 + x_3^T\hat{N}_3$$

$$y = y_1^T\hat{N}_1 + y_2^T\hat{N}_2 + y_3^T\hat{N}_3 \tag{119}$$

We have

$$\frac{\partial N_i}{\partial x} = \tag{120}$$

We need to find $\frac{\partial \xi}{\partial x}, \frac{\partial \xi}{\partial y}, \frac{\partial \eta}{\partial x}$ and $\frac{\partial \xi}{\partial y}$. Since $x = x(\xi,\eta)$ and $y = y(\xi,\eta)$, we get

$$\begin{bmatrix} dx \\ dy \end{bmatrix} = \begin{bmatrix} \frac{\partial x}{\partial \xi} & \frac{\partial x}{\partial \eta} \\ \frac{\partial y}{\partial \xi} & \frac{\partial y}{\partial \eta} \end{bmatrix} \begin{bmatrix} d\xi \\ d\eta \end{bmatrix} \tag{121}$$

The Jacobian of matrix is given by

$$|J| = \begin{vmatrix} \frac{\partial x}{\partial \xi} & \frac{\partial x}{\partial \eta} \\ \frac{\partial y}{\partial \xi} & \frac{\partial y}{\partial \eta} \end{vmatrix} = \begin{vmatrix} x_2^T - x_1^T & x_3^T - x_1^T \\ y_2^T - y_1^T & y_3^T - y_1^T \end{vmatrix} \tag{122}$$

And the inverse of (121) is given by

$$\begin{bmatrix} d\xi \\ d\eta \end{bmatrix} = \begin{bmatrix} \frac{\partial \xi}{\partial x} & \frac{\partial \xi}{\partial y} \\ \frac{\partial \eta}{\partial x} & \frac{\partial \eta}{\partial y} \end{bmatrix} \begin{bmatrix} dx \\ dy \end{bmatrix} = \frac{1}{|J|} \begin{bmatrix} \frac{\partial y}{\partial \eta} & -\frac{\partial x}{\partial \eta} \\ -\frac{\partial y}{\partial \xi} & \frac{\partial x}{\partial \xi} \end{bmatrix} \begin{bmatrix} dx \\ dy \end{bmatrix} \tag{123}$$

This gives us

$$\frac{\partial \xi}{\partial x} = \frac{1}{|J|}\frac{\partial y}{\partial \eta} \qquad \frac{\partial \xi}{\partial y} = \frac{1}{|J|}\frac{\partial x}{\partial \eta} \tag{124}$$

$$\frac{\partial \eta}{\partial x} = \frac{1}{|J|}\frac{\partial y}{\partial \xi} \qquad \frac{\partial \eta}{\partial y} = \frac{1}{|J|}\frac{\partial x}{\partial \xi} \tag{125}$$

It follows that

$$\frac{\partial N_1}{\partial x} = \frac{1}{|J|}(y_2^T - y_3^T) \qquad \frac{\partial N_1}{\partial y} = \frac{1}{|J|}(x_3^T - y_2^T) \tag{126}$$

$$\frac{\partial N_2}{\partial x} = \frac{1}{|J|}(y_3^T - y_1^T) \qquad \frac{\partial N_2}{\partial y} = \frac{1}{|J|}(x_3^T - x_1^T) \tag{127}$$

$$\frac{\partial N_3}{\partial x} = \frac{1}{|J|}(y_2^T - y_1^T) \qquad \frac{\partial N_3}{\partial y} = \frac{1}{|J|}(x_2^T - x_1^T) \tag{128}$$

All the terms in equations (126), (127) and (128) are constants, and the area of T is denoted by A_T. The element stiffness matrix for T is given by

$$K^T = A_T = \begin{bmatrix} \partial_x N_1^2 + \partial_y N_1^2 & \partial_x N_1 \partial_x N_2 + \partial_y N_1 \partial_y N_2 & \partial_x N_1 \partial_x N_3 + \partial_y N_1 \partial_y N_3 \\ \partial_x N_2 \partial_x N_1 + \partial_y N_2 \partial_y N_1 & \partial_x N_2^2 + \partial_y N_2^2 & \partial_x N_2 \partial_x N_3 + \partial_y N_2 \partial_y N_3 \\ \partial_x N_3 \partial_x N_1 + \partial_y N_3 \partial_y N_1 & \partial_x N_3 \partial_x N_2 + \partial_y N_3 \partial_y N_2 & \partial_x N_3^2 + \partial_y N_3^2 \end{bmatrix} \tag{129}$$

In the Laplace equation discussed here, we have chosen to use a constant load function $f = 1$. We make this choice so as to avoid problems that are not necessary in our final formulation.
We know that the entry F_i in the right-hand vector F is given by

$$F_i = l(\phi_i) = \int f\phi_i(x,y)dA = \int \phi_i(x,y)dA \qquad f = 1 \tag{130}$$

Since for the element matrix, ϕ_i is non-zero at the elements which share node i, we can also write the previous expression of the Jacobian as

$$F_{hi} = \sum_{k=1}^{s} \int N_i(x,y)dA \tag{131}$$

where S is the number of elements in Ω over which the support of N_i is unequal zero. Using the framework mapping between T and $\hat{T}$, we can define (131) in terms of reference coordinates (ξ, η). Using $dA = |detJ| \int \hat{N}_i(\xi,\eta)d\xi d\eta$ we get

$$F_{hi} = \sum_{k=1}^{S} \int \hat{N}_i(\xi,\eta)|detJ|d\xi d\eta = \sum_{k=1}^{S} |detJ| \int \hat{N}_i(\xi,\eta)d\xi d\eta \tag{132}$$

The Jacobian J is independent of the elements S. The integral in (132) is simply

$$\int \hat{N}_i(\xi,\eta) = \frac{1}{6} \qquad \forall i = 1,2,3 \tag{133}$$

So,

$$F_{hi} = \sum_{k=1}^{S} \int \hat{N}_i(\xi,\eta)|detJ|d\xi d\eta = \frac{1}{6}\sum_{k=1}^{S}|detJ| \tag{134}$$

The element matrix derived above is only for one element, we have as many 3×3 matrices as we have elements. To form the entire matrix, we need to place these element matrices at their proper positions. Similar working is repeated for the vector F. After putting the system together, we need to remove the columns and rows corresponding to boundary nodes, because there we have given function values, in our case $u = 0$ along the boundary. Then what follows is solving the system using the appropriate methods and then plotting it.

4.1.12 Summary

As we stated at the beginning, we associate a differential operator (say L) to every PDE. For instance, for the Poisson, $L = \nabla^2$. The Finite difference method discretizes this operator by replacing every differential with an approximate expression using differential formulas. It does this by making a grid of nodes, and uses the step length, which in general may vary between nodes to find expressions for these formulas. The Taylor series is very important in doing this.
The idea of discretization of the domain in which the PDE is defined is a common exercise for both FE an FD methods. We have nodes in both FE and FD.
The main difference of the two methods lies in the concept of approximation. FD discretizes the operator whereas FE discretizes the underlying domain X . Recall that in the FE method used in this work, we derived a weak formulation and based on it we defined a space of functions in which we supposed ours was to be found. that is

$$X = \{v \in H^1(\Omega) : v|_{\partial\Omega} = 0\} \tag{135}$$

and (136)

$$H^1(\Omega) = \{v : \Omega \longrightarrow R : \int_\Omega v^2, \int_\Omega v_x^2, \int_\Omega v_y^2 < \infty\} \tag{137}$$

X is an infinite dimensional space; there is an infinite number of functions that are zero on the boundary and quadratic integrable until first partial derivatives. In our example in this paper, we have used functions which are linear polynomials for each element. The solution is continuous across the element boundaries.

4.2 Discontinuous Galerkin method (DG)

Galerkin finite element methods are high order methods used to solve convection dominated PDEs. Since they make use of finite elements just like the FEM, they are efficient for use in domains having complex geometry. The discontinuous Galerkin finite element

methods makes use of discontinuous approximating functions and basis functions. This makes the methods explicit in nature such that the solution can be developed at element level hence allowing different orders of accuracy for each element. This is one of the advantages of the method over other numerical methods. Another advantage is that the resulting mass matrix is local to the cell which allows for an explicit time stepping and no systems to solve. Also, due to the localized nature of the method, it allows only communication between elements that share a common boundary. This in turn leads to efficient parallelization (Flaherty et. al). This feature implies that the mass matrix in this scheme is block diagonal hence easy to find its inverse. In addition, this method provides stable numerical solutions for first order PDEs. We therefore choose this method for use in this project.
The challenges that are encountered while using this method are that: It is more tedious as compared to the FD method and also it involves more degrees of freedom unlike the FV method.

4.2.1 Runge-Kutta Discontinuous Galerkin method (RKDG)

These are DG methods that applies Runge-Kutta methods at the point of time-discretization. They are used for solving non-linear hyperbolic PDEs especially non-linear conservation laws arising in:

- Shallow water models
- Gas dynamics models and
- Magneto-hydrodynamics models

4.2.2 Steps in the RKDG method

These are the steps followed in this method:

i. **Spatial discretization:** The domain in which we seek the solution is divided into a finite number of elements just as done in the FEM. Let us consider a non-linear hyperbolic conservation law of the form

$$u_t + \nabla f(u) = 0$$

The unknown **u** is approximated using a discontinuous piecewise smooth function U_h. We choose U_h such that it it contained in a finite dimensional space V_{DG}. Since this approximating function is not continuous across the interface between elements, we take in each element U_h^L and U_h^R to represent the left and right limits respectively.

ii. **Choice of basis functions:** This method gives freedom in the choice of the basis functions. Bokhove (2003), chooses the basis functions as the mean and slope of the approximating function. Cockburn (1998), uses Legendre polynomials P_l instead. In the solution of the 1D SWE in the following chapter, we use the Legendre polynomials as the approximating functions. The first four Legendre polynomials are given by:

$$P_0(x) = 1$$

$$P_1(x) = x$$

$$P_2(x) = \frac{1}{2}(3x^2 - 1) \tag{138}$$

$$P_3(x) = \frac{1}{2}(5x^3 - 3x)$$

iii. **Time discretization:** From the first two steps the conservative law stated in step (i) is reduced into an ODE of the form

$$\frac{d}{dt}U_h = R_h(U_h)$$

We then discretize this system in time using an explicit Runge-Kutta method (RK) which is achieved in three steps;

1. Set $U_h^0 = U_h^n$

2. For $i = 1, ..., K$ determine the functions between U_h^0 and U_h^n as

$$U_h^{(i)} = \sum_{i=0}^{i-1} \mu_{il}\omega_h^{il}, \qquad \text{where } \omega_h^{il} = U_h^{(l)} + \gamma_{il}\Delta t^n R_h(U_h^{(l)}) \tag{139}$$

3. Set $U_h^{n+1} = U_h^K$

The stability of these methods relies on this step i.e. it depends on the stability of the map

$$U_h^{(l)} \longmapsto \omega_h^{il} \tag{140}$$

This map may not always be stable. To enforce stability we use the last step described below

iv. **Slope limiter:** The generalized slope limiter methods involve reconstruction of the variables inside the elements using linear or quadratic elements. The standard representation of the slope limiter is $\bigwedge \prod_h^K$, Cockburn (1998). It is a non-linear projection operator designed such that $U_h^l = \bigwedge \prod_h v_h$ for some function v_h. If this holds then the mapping (141) is stable. The slope limiter algorithm is

1. Set $U_h^0 = U_h^n$
2. For $i = 1, ..., K$ determine the functions between U_h^0 and U_h^n as

$$U_h^{(i)} = \bigwedge \prod_h \sum_{i=0}^{i-1} \mu_{il} \omega_h^{il}$$

3. Set $U_h^{n+1} = U_h^K$

4.2.3 The general RKDG methods and their stability

In this section we give a detailed description of the steps stated above. We also elaborate on how the stability of the methods is enforced. The forward Euler step defined by the map (140) is not always stable in the L^2-norm. We are therefore going to come up with a weaker stability property for this operator and enforce it with the general slope limiter to obtain a stable method.

The DG-spatial discretization

This method is locally conservative and has order $k + \frac{1}{2}$ if polynomials of degree k are used. The resulting mass matrix in this step is a block diagonal which guarantees the method to be highly parallelisable. Again the numerical trace $\hat{f}$ relies on the traces of u_h on either side of the interface of any two elements. The choice of the numerical trace is usually very delicate and a crucial aspect of the definition of the DG methods as it can affect their consistency, stability and accuracy. Consistency of the method holds that the approximate solution U_h can be replaced with the exact solution u in the weak formulation without affecting the formulation. This means that the numerical trace U_h should be chosen in a way such that $\hat{U} = u$.
Let us consider the initial value problem

$$\frac{d}{dt}u(t) = f(t)u(t), \qquad t \in [0,T], \qquad u(0) = u_0 \tag{141}$$

We want to find the approximate solution U_h on $[0,T]$. We begin by first partitioning the time interval $(0,T)$ into $\{t^n\}_{n=0}^N$ partitions and set $I_n = (t^n, t^{n+1}) \qquad n = 0, 1, ..., N-1$. We then identify a function U_h on I_n which is a polynomial of degree not greater than k^n, multiply the equation by this function then integrate over I_n

$$\int_{I_n} u_h(s) \frac{d}{dt} v(s) ds = \hat{u}_h v|_{t^n}^{t^{n+1}} = \int_{I_n} f(s)u(s)v(s)ds \tag{142}$$

where $v(s)$ is a test function and

$$\hat{U}_h(t^n) = \begin{cases} u_0, & t^n = 0 \\ \lim_{\varepsilon \downarrow 0} U_h(t^n - \varepsilon), & \text{otherwise} \end{cases}$$

4.2.4 Stability

Still considering the ODE (141), if we multiply through by u and integrate over the entire time interval we obtain

$$\frac{1}{2}u^2(T) - \frac{1}{2}u_0^2 = \int_{[0,T]} f(s)u^2(s)ds \tag{143}$$

This represents the L^∞-stability of the solution. For the DG method, let us choose a test function $v = u_h$ in the weak formulation Eq (142). Integrating by parts yields

$$\sum_{n=0}^{N-1}(-\frac{1}{2}u_h^2 + \hat{u_h}u_h)|_{t^n}^{t^{n+1}} = \frac{1}{2}u_h^2(T^L) + \Theta_h(T) - \frac{1}{2}u_0^2 = \int_0^T f(s)u_h^2(s)ds \tag{144}$$

with

$$\Theta_h(T) = -\frac{1}{2}u_h^2(T^L) + \sum_{n=0}^{N-1}(-\frac{1}{2}u_h^2 + \hat{u_h}u_h)|_{t^n}^{t^{n+1}} + \frac{1}{2}u_0^2$$

The stability of the DG methods holds if

$$\Theta_h(T) \geq 0$$

. Let us set

$$\begin{aligned} u_h(t) &= u_0, \qquad t < 0 \\ \{u_h\} &= \frac{1}{2}(u_h^L + u_h^R) \\ [u_h] &= u_h^L - u_h^R \\ u_h^{L,R} &= \lim_{\varepsilon \downarrow 0} u_h(t \pm \varepsilon) \end{aligned}$$

then

$$\Theta_h(T) = -\frac{1}{2}u_h^2(T^L) + (\frac{1}{2}u_h^2(T^L) + \hat{u}_h(T)u_h(T_L)) + \sum_{n=0}^{N-1}(-\frac{1}{2}[u_h^2] + \hat{u}_{h[u_h]})t^n$$

$$-(-\frac{1}{2}u_h^2(0^R) + \hat{u}_h(0)u_h(0^R) + \frac{1}{2}u_0^2$$

$$= (\hat{u}_h(T) - u_h(T^L))u_h(T^L) + \sum_{n=1}^{N-1} ((\hat{u}_h - \{u_h\}[u_h])(t^n)$$

$$-(\hat{u}_h(0) - u_0)u_h(0^R) + \frac{1}{2}[u_h]^2(0) \tag{145}$$

where $[u_h^2]$ is an identity.
Then defining the trace

$$\hat{u}_h(t^n) = \begin{cases} u_0, & \text{at } t^0 = 0 \\ (\{u_h\} + C^n[u_h])t^n, & \text{if } t^n \in [0,T] \\ u_H(T^L), & t^n = T \end{cases}$$

for C^n non-negative and setting $C^0 = \frac{1}{2}$ we have from (144)

$$\Theta_h(T) = \sum_{n=0}^{N-1} C^n[u_h]^2(t^n) \geq 0 \tag{146}$$

This is the condition for numerical stability which is dependent on the numerical trace u_h

The RK-time discretisation

Let us consider the definition of the intermediate function given in (139). Let us choose non-zero values for both μ_{il} and γ_{il} and let $\mu_{il} \geq 0$ satisfying that $\sum_{l=0}^{i-1} \mu_{il} = 1$. Using these conditions and assuming that for a semi-norm $|.|$, we have that

$$|\omega_h^{il}| \leq |u_h^{(l)}| \tag{147}$$

then

$$|u_h^{(i)}| = |\sum_{l=0}^{i-1} \mu_{il}\omega_h^{il}|, \qquad \text{by 139}$$

$$\leq \sum_{l=0}^{i-1} \mu_{il}|\omega_h^{il}|, \qquad \text{by the positivity of } \mu_{il}$$

$$\leq \sum_{l=0}^{i-1} \mu_{il}|u_h^{(l)}| \qquad \text{by stability of 147}$$

$$\leq \max_{0\leq l\leq i-1} |u_h^{(l)}| \qquad \text{by the consistency property}$$

From this we obtain that $|u_h^n| \leq |u_h^0|$ for all $n \geq 0$ (by induction). This indicates that the stability of the Euler forward step (140) implies the stability of the RK method.

4.2.5 Round-off errors

The RK approach is explicit and may result to amplification of round-off errors. This defect has to be controlled by using some conditions in order to retain the accuracy of the method. For the one-dimensional linear case $f(u) = cu$ for example, a von Neumann stability analysis gives a stability of

$$|c|\frac{\triangle t}{\triangle x} \leq \frac{1}{2k+1} \tag{148}$$

for a $k+1$-stage RK method where k is the degree of the approximating polynomials in the DG discretization.

Stability of the step $u_h \longmapsto \omega_h = u_h + \delta R_h(u_h)$

The map (140) is not stable in the L^2-norm except in the situation where polynomials of degree 0 are used. Otherwise, if the polynomials are not constants, the forward Euler step (140) can only be stable if $\frac{\triangle t}{\triangle x}$ is proportional to $(\triangle x)p(k)$ for $p(k) > 0$ e.g. $p(1) = \frac{1}{2}$, Chavent G. and Cockburn B. (1989). This condition can only apply where hyperbolic problems are involved. To deal with this situation, weaker norms or semi-norms were introduced for which the Euler step would satisfy stability. To illustrate this let us use the one dimensional case and define the Euler step (140) as follows

$$\int_{I_j} \frac{(\omega_h - u_h)}{\delta t} v_h dx - \int_{I_j} f(u_h)(v_h)_x dx + \hat{f}(u_h)v_h|_{x_{j-\frac{1}{2}}}^{x_{j+\frac{1}{2}}} = 0 \tag{149}$$

Using $v_h = 1$ we get from (149)

$$(\bar{\omega}_j - \bar{u}_j)/\delta t + (\hat{f}(u^L_{j+\frac{1}{2}}, u^R_{j+\frac{1}{2}}) - \hat{f}(u^L_{j-\frac{1}{2}}, u^R_{j-\frac{1}{2}}))/\triangle_j = 0 \tag{150}$$

where $\bar{u_j}$ is the mean of u_h in I_j, $u^L_{j+\frac{1}{2}}$ and $u^R_{j+\frac{1}{2}}$ are the left and right hand side limits of u_h in I_j respectively. Using a piecewise constant approximating function u_h we get a monotone scheme for small enough values of δ and as a result the scheme will be total variation diminishing (TVD) i.e.

$$|\bar{\omega}_h|_{TV(0,1)} \leq |\bar{u}_h|_{TV(0,1)} \tag{151}$$

where $|\bar{u}_h|_{TV(0,1)} \equiv \sum_{1 \leq j \leq N} |\bar{u}_{j+1} - \bar{u}_j|$ denotes the total variation of the local means.
If the approximate solutions are not piecewise constant, then for (151) to hold we require that

$$sign(u^R_{j+\frac{1}{2}} - u^R_{j-\frac{1}{2}}) = sign(\bar{u}_{j+1} - \bar{u}_j)$$

$$sign(u^L_{j+\frac{1}{2}} - u^L_{j-\frac{1}{2}}) = sign(\bar{u}_j - \bar{u}_{j-1}) \tag{152}$$

The conditions (152) are not necessarily satisfied hence we have to use the generalized slope limiter $\bigwedge\prod_h$ to enforce them, Cockburn B. (2001).

4.2.6 The generalized slope limiter

This is a technique used to construct a TVD method. It involves reconstruction of the variables inside an element by use of linear or quadratic functions, Cockburn (1998). For piecewise linear functions

$$v_h|_{I_j} = \bar{v}_j + (x - x_j)v_{x,j}, \tag{153}$$

we define the slope limiter of v_h as

$$u_h|_{I_j} = \bar{v}_j + (x - x_j)m(v_{x,j}, \frac{\bar{v}_{j+1} - \bar{v}_j}{\triangle_j/2}, \frac{\bar{v}_j - \bar{v}_{j-1}}{\triangle_j/2}) \tag{154}$$

where

$$m(\alpha_1, \alpha_2, \alpha_3) = \begin{cases} s\min_{1\le n\le 3}|\alpha_n|, & \text{if } s = sign(\alpha_1) = sign(\alpha_2) = sign(\alpha_3) \\ 0, & \text{otherwise} \end{cases}$$

is a midmod function. We can re-write the non-linear projection (154) as

$$u^L_{j+\frac{1}{2}} = \bar{v}_j + m(v^L_{j+\frac{1}{2}} - \bar{v}_j, \bar{v}_j - \bar{v}_{j-1}, \bar{v}_{j+1} - \bar{v}_j) \tag{155}$$

$$u^R_{j-\frac{1}{2}} = \bar{v}_j - m(\bar{v}_j - v^R_{j-\frac{1}{2}}, \bar{v}_j - \bar{v}_{j-1}, \bar{v}_{j+1} - \bar{v}_j) \tag{156}$$

For general discontinuous functions denote by v^1_h the L^2-projection of v_h into the space of piecewise linear functions. Then on I_j the approximation u_h is modified as

$$u_h = \bigwedge\prod_h(v_h) \tag{157}$$

Then

i. compute $u^L_{j+\frac{1}{2}}$ and $u^R_{j-\frac{1}{2}}$ using (155) and (156)

ii. If $u^L_{j+\frac{1}{2}} = v^L_{j+\frac{1}{2}}$ and $u^R_{j-\frac{1}{2}} = v^R_{j-\frac{1}{2}}$ set $u_h|_{I_j} = v_h|_{I_j}$

iii. If (ii) doesn't apply take $U_h|I_j = \bigwedge\prod^1_h(v^1_h)$

This enforcement of sign conditions stabilizes the forward Euler step In the next chapter we apply the Discontinuous Galerkin Finite element method to solve the one-dimensional shallow water equation.

5 The DG for solving the 1D SWE

In this chapter we make use of the RKDG to solve the 1D SWE (84). We opt to use this method due to the following reasons;

i. It combines some properties from the FDM and FEM resulting to a high accuracy.

ii. It is suitable for complex geometries.

iii. It is well adapted to parallelization hence easy to use.

iv It can capture discontinuities without generating spurious oscillations.

The 1D shallow water equation in its conservation law form (84) has to be discretized both in space, x and time, t. The spatial discretization is done by considering linear finite elements in which the unknown $u(x,t)$ is approximated by use of discontinuous piecewise polynomials. We take our basis functions to be the Legendre polynomials P_l in this case and the time discretization is done using the Runge-Kutta method.

5.0.1 Spatial discretization

The linear interval $J=[x_0,x_N]$ is divided into a finite number of subintervals $J_i=[x_{i-\frac{1}{2}},x_{i+\frac{1}{2}}]$. The unknown is then approximated using piecewise smooth functions $\breve{U}(x,t)$ which are not continuous between elements. These functions belong to the discontinuous Galerkin finite element space defined by

$$V_G=\{v\in L^1(J)|u\in p^n(J_i),\forall I_i\in J\} \tag{158}$$

where $L^1(J)$ is the space of Lebesque integrable functions on I and $p^n(J_i)$ is the space of polynomials in J_i of degree n.
We choose the Legendre polynomials as our basis functions. This choice has also been used by Schwanenberg (2003). The Legendre polynomials are usually orthogonal in L^2 and we have on the interval $[-1,1]$ that

$$\int_{-1}^{1}p_l(r)p_m(r)dr=\frac{2}{2l+1}\delta_{lm} \tag{159}$$

where $\delta_{lm}=\begin{cases}1, & l=m\\ 0, & l\neq m\end{cases}$ is the Kronecker delta. This orthogonality is what we apply to get a diagonal mass matrix M. The general form of the approximating function $\breve{U}(x,t)$

is then given by

$$\check{U}(x,t) = \sum_{l=0}^{n} u_i^l(t)\psi_i^l(x), \qquad x \in [x_{i-\frac{1}{2}}, x_{i+\frac{1}{2}}] \tag{160}$$

where

$$\psi_i^l(x) = P_l(\frac{2(x-x_i)}{h_i}) \tag{161}$$

are the basis functions, $h_i = x_{i+\frac{1}{2}} - x_{i-\frac{1}{2}}$ and $x_i = \frac{x_{i+\frac{1}{2}} - x_{i-\frac{1}{2}}}{2}$. This approach gives us an approximate for u in each element in terms of degree n polynomials. We end up with $n+1$ unknowns which are the coefficients $u_i^l, l = 0,1,...,n$. Using the N elements the matrix of coefficients is of the order $N \times (n+1)$.

5.0.2 The weak formulation

The weak formulation of the 1D SWE (84) is obtained by first multiplying it by a test function $\xi \in \eta$ and integrating over the interval J_i. Here η is a suitable functional space

$$\int_{J_i} (\frac{\partial u}{\partial t}\xi + \frac{\partial}{\partial x} f(u)\xi - s(u)\xi)dx = 0$$

since the approximates $\check{U}(x)$ are linearly independent of each other, then for each element J_i we have

$$\int_{x_i-\frac{1}{2}}^{x_i+\frac{1}{2}} (\frac{\partial u}{\partial t}\xi + \frac{\partial}{\partial x} f(u)\xi - s(u)\xi)dx = 0$$

or for the N elements the sum

$$\sum_{i=0}^{N} [\int_{x_i-\frac{1}{2}}^{x_i+\frac{1}{2}} (\frac{\partial u}{\partial t}\xi + \frac{\partial}{\partial x} f(u)\xi - s(u)\xi)dx] = 0 \tag{162}$$

Integrating the second term of this integral by parts we have

$$\int \frac{\partial f}{\partial x}\xi dx = \int \xi \frac{\partial f(u)}{\partial x}dx = f(u)\xi|_{x_i-\frac{1}{2}}^{x_i+\frac{1}{2}} - \int f(u)\frac{\partial \xi}{\partial x}dx$$

Using this in (162) we obtain

$$\sum_{i=0}^{N} [\int_{x_i-\frac{1}{2}}^{x_i+\frac{1}{2}} \xi \frac{\partial u}{\partial t}dx + f(u)\xi|_{x_i-\frac{1}{2}}^{x_i+\frac{1}{2}} - \int_{x_i-\frac{1}{2}}^{x_i+\frac{1}{2}} f(u)\frac{\partial \xi}{\partial x}dx - \int_{x_i-\frac{1}{2}}^{x_i+\frac{1}{2}} s(u)\xi dx] = 0 \tag{163}$$

Eq (163) is the weak formulation of the equation (84). In this form we only require $f(u)$ to be integrable unlike in the strong formulation form where we required it to be continuously

differentiable. This is the advantage of the weak formulation. Note that the approximate $\check{U}$ of u has two different values in each element. Thus for the flux $f(\check{U})$, we approximate it using

$$F(\check{U}(x_{i+\frac{1}{2}},t)) = F(\check{U}^L(x_{i+\frac{1}{2}},t),\check{U}^R(x_{i+\frac{1}{2}},t)) \tag{164}$$

where $\check{U}^L$ and $\check{U}^R$ represents the left and the right limits of $\check{U}$ respectively at the nodes where $\check{U}$ has a discontinuity. Recall that we put that $\check{U}$ is contained in the space defined by (158). We choose the weighted functions used to derive the weak formulation to be contained in the same functional space. Again we take the test function to be similar to the basis functions, so $\xi = \psi_i^m(x)$ where $m = 0,1,...,l$. Using the new form of our function in (163) we get for each element J_i

$$\int_{x_i-\frac{1}{2}}^{x_i+\frac{1}{2}} \{\partial_t \sum_{l=0}^{n} u_i^l \psi_i^l\} \psi_i^m dx - \int_{x_i-\frac{1}{2}}^{x_i+\frac{1}{2}} f(\check{U}) \psi_i'^m dx - \int_{x_i-\frac{1}{2}}^{x_i+\frac{1}{2}} s(\check{U}) \psi_i^m dx$$

$$+F(\check{U}(x_{i+\frac{1}{2}},t)) - (-1)^m F(\check{U}(x_{i-\frac{1}{2}},t)) = 0 \tag{165}$$

where the prime on the second integral denotes differentiation with respect to x and we used $\psi_l(x_{i+\frac{1}{2}}) = P_l(1) = 1$ and $\psi_l(x_{i-\frac{1}{2}}) = P_l(-1) = (-1)^l$. From (165)

$$\int_{x_i-\frac{1}{2}}^{x_i+\frac{1}{2}} \partial t \{\sum_{l=0}^{n} u_i^l \psi_i^l\} \psi_i^m dx = \partial_t (\sum_{l=0}^{n} [u_i^l \int_{x_i-\frac{1}{2}}^{x_i+\frac{1}{2}} \psi_i^l \psi_i^m dx])$$

$$= \sum_{i=0}^{n} \int_{-1}^{1} \psi_i^l \psi_i^m \frac{du_i^l}{dt} dx$$

$$= \frac{h_i}{2m+1} \frac{du_i^m}{dt} \tag{166}$$

where we applied the orthogonality relation of Legendre polynomials (159) and the definition (161). As a consequence of this result, we end up with a diagonal mass matrix which we have to solve.
Using (166) in (167), we find for $i = 1,\cdots,N$ and for $l = 0,\cdots,n$ that

$$\dot{u}_i^l = \frac{2l+1}{h_i}[\int_{x_i-\frac{1}{2}}^{x_i+\frac{1}{2}} f(\check{U}) \psi_i'^l dx + \int_{x_i-\frac{1}{2}}^{x_i+\frac{1}{2}} S(\check{U}) \psi_i^l dx] - \frac{2l+1}{h_i}[F(\check{U}(x_{i+\frac{1}{2}},t)) -$$

$$(-1)^l F(\check{U}(x_{i-\frac{1}{2}},t))] \tag{167}$$

where the dot indicates differentiation with respect to t. This is an ODE of the form

$$\frac{d}{dt}\check{U}_h = R_h(\check{U}_h) \tag{168}$$

with $\check{U}_h$ defined by

$$\check{U}_h = \begin{bmatrix} u_1^0 & u_1^1 & \cdots & u_1^n \\ u_2^0 & u_2^1 & \cdots & u_2^n \\ \vdots & \vdots & & \vdots \\ u_N^0 & u_N^1 & \cdots & u_N^n \end{bmatrix} \tag{169}$$

and R_h is a vector made up of the R.H.S of the equation. We applied the Gauss quadrature formula to find the values of the integrals contained in R_h. The quadrature formula state that

$$\int_\alpha^\beta g(x)dx \cong \sum_{i=1}^{q} \xi_i g(\lambda_i), \qquad \alpha \leq \lambda_i \leq \beta \tag{170}$$

where λ_i are called Gauss points. Using $q = 3$, we make a three point approximation. The basis functions are constants. For instance, when $n = 0$ the equation (167) becomes

$$\dot{U}_i^0 = -\frac{1}{\triangle\, x_i}[F(U_i^0, U_{i+1}^0) - F(U_{i-1}^0, U_i^0)] + S_i \tag{171}$$

where $F(U_i^0, U_{i+1}^0)$ is the flux between elements i and $i+1$ and $S_i = \frac{1}{\triangle x_i}\int_{x_{i-\frac{1}{2}}}^{x_{i-\frac{1}{2}}}$

The DG scheme is said to be monotone if $\mathbf{F}(U^L, U^R)$ is locally Lipsichitz, consistent and monotone. The Harten-Lax-Van Leer (HLL) scheme, Harten et. al accounts for the left and right characteristics. This consideration separates the the flux into three states

$$\mathbf{F}^{HLL}(U^L, U^R) = \begin{cases} \mathbf{F_L}, & \text{if } \lambda_{min} \geq 0 \\ \mathbf{F}^*, & \text{if } \lambda_{min} < 0 \lambda_{max} > 0 \\ \mathbf{F_R}, & \text{if } \lambda_{max} \leq 0 \end{cases} \tag{172}$$

where $\mathbf{F_L} = \mathbf{F}(\mathbf{U_L}), \mathbf{F_R} = \mathbf{F}(\mathbf{U_R})$ and $\mathbf{F}^* = \frac{\lambda_{max}\mathbf{F_L} - \lambda_{min}\mathbf{F_R} + \lambda_{max}\lambda_{min}(\mathbf{U^R} - \mathbf{U^L}}{\lambda_{max} - \lambda_{min}}$

The rarefaction waves determine the wave speeds

$$\lambda_{min} = min(u^L - \sqrt{gh^L}, u^* - \sqrt{gh^*})$$

$$\lambda_{max} = max(u_R - \sqrt{gh^R}, u^* + \sqrt{gh^*})$$

where

$$u^* = \frac{u^L + u^R}{2} + \sqrt{gh^L} - \sqrt{gh^R}$$

$$\sqrt{gh^*} = \frac{u^L - u^R}{4} + \frac{\sqrt{gh^L} + \sqrt{gh^R}}{2}$$

Time discretization

Time in this work is discretized using the Runge-Kutta method (RK). Let us consider the initial condition $u(x,0)$ at $t=0$. The initial approximation at this point is then given by U_{h0}. The time interval $[0,T]$ is to be discretized into $\{t^k\}_{k=0}^{K}$, where T is the total time of computation and $\triangle t^k = t^{k+1} - t^k$, $k = 0,1,\cdots,K-1$
Let us denote $U_h^0 = U_{h0}$ as the initial polynomial approximation. Then we can use iteration methods to find U_h^{k+1} from U_h^n. If we choose $i = 1,\cdots,(m+1)$ and using RK methods of the order $(m+1)$ then

$$U_h^j = (\sum_{l=0}^{j-1} \mu_{jl} U_h^l + \gamma_{jl} \triangle t^k R_h(U_h^l)) \tag{173}$$

Using the Runge-Kutta method of the first order

$$U_h^{k+1} = \mu_{1,0} U_h^k + \gamma_{1,0} \triangle t^k R_h(U_h^k))$$

$$= U_h^k + \triangle t^k R_h(U_h^k) \tag{174}$$

A second order R-K method will be sufficient here since our basis functions are linear
Let us again denote the CFL-number by ζ. This number expresses the relationship of the speed of the wave propagation in the actual domain and the grid speed. If $\triangle x$ is a spatial grid variation within a time $t = \triangle t$, the grid speed is given by $\frac{\triangle x}{\triangle t}$. In this case we are using a linear domain J_i so we define

$$\zeta = \frac{\triangle t}{\triangle x}(|v| + c) \tag{175}$$

where c is the wave speed. This gives

$$\triangle t = \zeta \frac{\triangle x}{(|v| + c)} \tag{176}$$

The CFL-number ζ is non-negative and bounded above by 1. It is maximum for $n = 0$ and decreases as the order of k increases. The table below shows the values of ζ used here
Sometimes the numerical solution $U(x)$ at times may display unphysical oscillations. To avoid this, we use the total variational diminishing (TVD) method. These methods allows us to restrict the total variation which eliminates the oscillations. We define (for u continuous)

$$TV(u) = \lim_{\sigma \longrightarrow 0} \sup \frac{1}{\sigma} \int_{-\infty}^{\infty} |u(x+\sigma) - u(x)| dx \tag{177}$$

If $u^k = \{u_i^k$ is a discrete function

$$TV(u^k) = \sum_{i=-\infty}^{\infty} |u_{i+1}^k - u_i^k| \tag{178}$$

If the initial condition $u(x,0)$ has bounded total variation then the exact solution of the exact scalar conservation law

$$\partial t(u) + \partial_x f(u) = 0$$

has the property that

i. We cannot possibly create a new extrema in x

ii. The lower bound of the exact solution does not decrease and the upper bound does not increase.

From these properties we see that $TV(u(t))$ is a decreasing function i.e.

$$TV(u(t_1)) \leq TV(u(t_2)), \qquad \forall t_1 \leq t_2$$

The numerical scheme is then termed as a Total Variation Diminishing scheme (TVD) and it holds that

$$TV(u^{k+1}) \leq TV(u^k), \qquad \forall k \tag{179}$$

The first order RKDG method satisfies this condition. We can extend this property to the 1D SWE by applying it to all the variables separately. In this work we use the slope limiter technique to construct the TVD for the 1D SWE used in this project. Slope limiting in the DG methods involves construction of the variables in each element using functions of the first order or the second order. We modify our solution technique in a way that it will satisfy the TVD property when $k > 1$.
Let us consider the linear part of our approximating function $U(x,t)$ by

$$U(x,t) = \sum_{l=0}^{1} u_i^l(t)\psi_i^l(x) \tag{180}$$

such that the coefficients matrix will be

$$V_h = \begin{bmatrix} u_1^0 & v_1^1 \\ u_1^0 & v_1^1 \\ \vdots & \vdots \\ u_N^0 & v_N^1 \end{bmatrix}$$

Let $\bigwedge\prod_h^k$ be the slope limiter, Cockburn (1998). We define the limit of U_h as $U_{lim} = \bigwedge\prod_h^k(U_h)$ where we apply the slope limiter separately to all the characteristic variables since we are dealing with a PDE system. We apply the following algorithm to determine $u^0_{lim,i}$ and $u^i_{lim,i}$ for $i = 1,...,N$

i. Find the transformed variables using the definition below

$$v_i^1 = B^{-1}u_i^1$$

$$v_i^L = B^{-1}(u_i^0 - u_{i-1}^0)$$
$$v_i^R = B^{-1}(u_{i+1}^0 - u_i^0)$$

where $B = \begin{bmatrix} 0 & 1 \\ \sqrt{gH_i^0} - (q_i^0/H_i^0)^2 & 2q_i^0/H_i^0 \end{bmatrix}$

ii. Obtain the limiting case v_i^1 as follows $v^1_{lim,i} = m(v_i^1, v_i^L, v_i^R)$ where
$m(\alpha_1,\alpha_2,\alpha_3) = \begin{cases} sign(\alpha_1)\min_{1\le n\le 3}|\alpha_n|, & sign(\alpha_1) = sign(\alpha_2) = sign(\alpha_3) \\ 0, & otherwise \end{cases}$
is the minmod function

iii. Reconvert the variables $v^1_{lim,i}$ to obtain the limited variable u_i^1. Note that u_i^0 is not modified since only the slope is limited

$$u^0_{lim,i} = u_i^0$$

$$u^1_{lim,i} = Bv^1_{lim,i}$$

and we get

$$V_{lim} = \begin{bmatrix} v^0_{lim,1} & v^1_{lim,1} \\ v^0_{lim,2} & v^1_{lim,2} \\ \vdots & \vdots \\ v^0_{lim,N} & v^1_{lim,N} \end{bmatrix}$$

Equation (173) becomes

$$U_h^j = \bigwedge\prod_h^k\Big(\sum_{l=0}^{j-1}\mu_{jl}U_h^l + \gamma_{jl}\triangle t^k R_h(U_h^l)\Big) \tag{181}$$

This results to the modification of the RK time discretization, Cockburn (1998).

5.1 Practical problem: The dam break problem

In nearly all countries of the world, hydroelectric power is the main source of the energy used for industrial processes, lighting among other uses. This power is generated in power stations where a dam is constructed along a water pathway such as a river. The water behind the dam possesses potential energy. This energy is used to rotate turbines in the process of power generation. To cater for the growing need of electricity, dams have to be made higher and stronger so that more water can be held behind the dam. The pressure of the water held behind the dam poses a danger of the dam breaking. A one dimensional dam-break physically represents an instantaneous collapse of an infinitesimal thin dam wall in a wide infinitely long horizontal channel. We will use the dam fail problem to test our solution in a channel of a finite water depth at each point downstream of the wall. If proper measures are not taken for risk management, a dam failure may cause loss of lifes and property. Therefore the risk of the dam breaking need to be assessed, in terms of;

1. The amount of water that will stream over the broken dam,
2. The speed with which the water will flow downstream
3. The water levels that are expected downstream

Knowing these will allow proper measures to be taken for protection. The water flow after a dam breaks can be described using the shallow water equations, J.J. Stoker, "Water Waves". The dependent variables are the water height, H and velocity, v and the only depend on the distance x and time, t. We assume an initial no flow condition and that the water domain is deeper in the dam at the right than at the left. If the dam breaks at a time $t_0 = 0$, the water begins to flow rightwards. Two types of waves are generated by this dam fail; a shock wave is propagated to the right while a rarefaction is propagated to the left. This leaves a constant water level in between.

5.1.1 Boundary conditions

The boundary conditions of the 1D domain (channel flow) are obtained by considering the left and right boundaries. We take the fluid flow in the left to be inwardly directed and on the right boundary to be outwardly directed. From equations (42) and (43) the 1D SWE can be expressed in its quasi-linear form as

$$\partial_t \mathbf{u} + B\partial_x \mathbf{u} = s(\mathbf{u}) \tag{182}$$

where $B = \frac{df}{du} = \begin{bmatrix} 0 & 1 \\ -\frac{q^2}{H^2} + gH & \frac{2q}{H} \end{bmatrix} = \begin{bmatrix} 0 & 1 \\ c^2 - u^2 & \end{bmatrix}$ is the Jacobi matrix and c the celerity.
The eigenvalues for B are

$$\lambda_1 = u - c$$
$$\lambda_2 = u + c$$

and the corresponding eigenvectors are

$$V_1 = \frac{H}{2c}\begin{bmatrix} 1 \\ u-c \end{bmatrix} \qquad \text{and} \qquad V_2 = \frac{H}{2c}\begin{bmatrix} 1 \\ u+c \end{bmatrix}$$

so that B is then diagonalizable as

$$B = RPR^{-1} \tag{183}$$

where $P = \begin{bmatrix} \lambda_1 & 0 \\ 0 & \lambda_2 \end{bmatrix}$ is the diagonal matrix and $R = (R_1, R_2)$.
Multiplying (181) by R^{-1} and using (182) yields

$$R^{-1}\partial_t u + PR^{-1}\partial_x u = R^{-1}s \qquad \text{or} \tag{184}$$
$$\partial_t \mathbf{r} + P\partial_x \mathbf{r} = \hat{s} \tag{185}$$

where $\hat{s} = R^{-1}s$ and $\mathbf{r} = \begin{bmatrix} r_1 \\ r_2 \end{bmatrix} = \begin{bmatrix} u - 2c \\ u + 2c \end{bmatrix}$ are characteristic variables called Riemann invariants. Equation (184) is the characteristic form of the 1D SWE. The characteristics of the eigenvalues determines the direction of the characteristics along which the information is conveyed. At this point, the boundary conditions are dependent on the Riemann invariants $u \pm 2u$.

We write a MATLAB program that solves the dam break problem. The Codes of the work are written in the Appendix page. These commands are used to obtain values of the solutions H and v for different time points and plot the graphs representing the information. The output of these numerical values of height and velocity is 300 for each variable and hence we have not included them in this work so as to safe space. We use a height, $H \in [0m, 6m]$ and an horizontal stretch $x \in [0m, 1000m]$. We choose $N - 1 = 400$ and $t \in [0, T]$ where the period $T = 70s$.
We consider the domain $\Omega = [-D, D]$ which has a length of $1000m$ and the Dirichlet boundary conditions $h(-D,t) = h_L, h(D,t) = h_R$ with $h_L \geq h_R$. The initial conditions are

$$h(x,0) = \begin{cases} h_L, & \text{if } 0 \leq x \leq 300 \\ h_R, & \text{if } 300 < x \leq 1000 \end{cases}$$

$$u(x,0) = 0 \qquad 0 \leq x \leq 1000 \tag{186}$$

with $h_L > h_R$. This is the Riemann problem for our homogeneous problem. We will compare our solution with the analytical solution derived by Stoker, 1957. The upstream depth h_L is maintained at $6m$ while the downstream depth is a variant. This leads to two different cases of flow:

1. $\frac{h_R}{h_L} > 0.5$, a subcritical flow
2. $\frac{h_R}{h_L} << 0.5$, a supercritical flow

In a subcritical flow, the fluid velocity is less than the wave velocity. In the first case, let us choose $h_R = 3.6$ and $h_L = 6$. The ratio of h_R to h_L gives $\frac{h_R}{h_L} = 0.6$, which describes a subcritical flow. The flow profile is then as shown in the graphs below, with the first plot showing the variation of H versus x and another for the velocity v versus x. A rarefaction occurs between 300 and $450m$ and a shock occurs downstream at $650m$. This is due to subcritical flow.

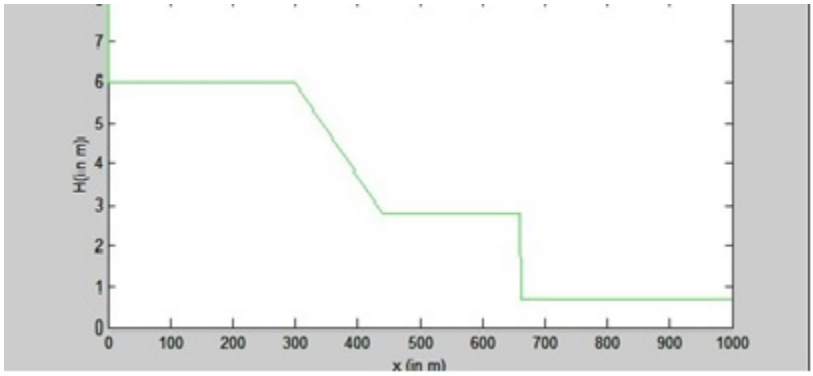

Fig 1: Variation of height with distance, x after Dam-break

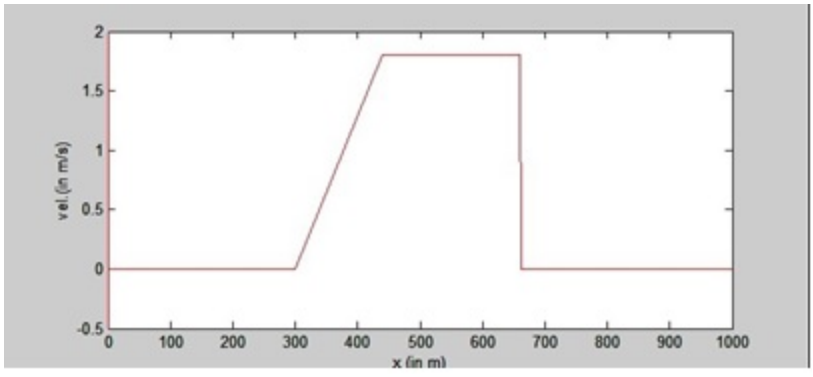

Fig 2: Velocity variation with distance, x after Dam-break (subcritical flow)

In the supercritical flow, let us take $h_R = 0.48$ and $h_L = 6$, then we have $\frac{h_R}{h_L} = 0.08$. The graphs below show the simulation of the flow profile for both height and velocity of water for the dam break.

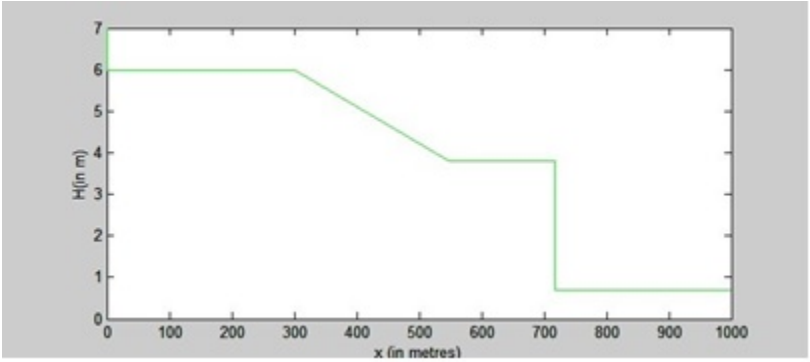

Fig 3: Variation of height with distance, x after Dam-break (supercritical flow)

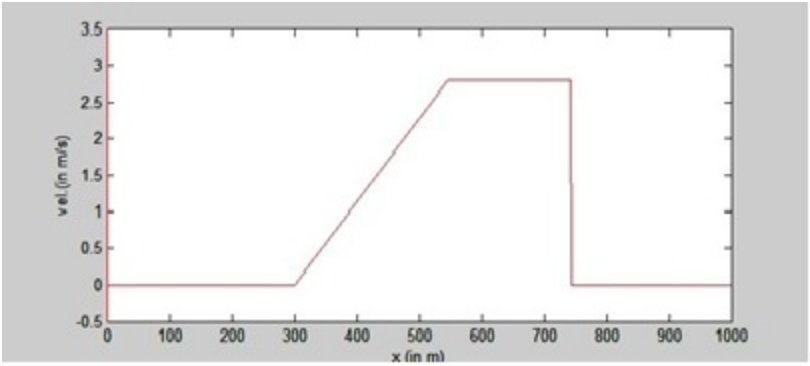

Fig 4: Variation of velocity with distance, x after Dam-break (supercritical flow)

The rarefactions are much steeper and longer in this case whereas the shock is formed much faster as compared to the previous case. This is because the flow is supercritical downstream i.e. the velocity of the fluid is much greater than the velocity of the gravity waves.

6 Results, Conclusions and Recommendations

6.1 Results

If a village is located a distance 1 kilometer downstream for example from the dam, dam experts want to know how long it will take for the flood to reach the village in case the dam fails. The height h of the water and the velocity v of flow at different points are dependent on the distance x along the flow and time t.
The domain of obtaining the solution contains the reservoir the channel and the village. We imposed a left boundary at $x = 0$. This is justified because the sides of the channel are steep. The right hand boundary is not clear. To find how long it takes the flood water to reach the village, we need to calculate the grid index for the village. This is dependent on the number of grids used in the domain. The Lax-Friedrich's scheme gives the following results

Number of Grids (N)	time(seconds)
100	308
200	369
400	402
800	414
1600	420
3200	423
6400	424

Table 1: Flood times for different grid sizes

A grid independent solution is obtained using 6400 grid points. The flood takes 7 minutes to reach the village. This indicates that if a dam breaks, the people at the village downstream have 7 minutes until the flood arrives.

6.1.1 Conclusion

The shallow water equations has a much more potential than is discussed in this work. They are well suited for tsunami wave wave modeling. They are used by tsunami warning

centers to model the tsunami wave propagation. Also, many hydrodynamical phenomena such as storm surges, river flooding and dam fail problem have been effectively treated using the shallow water theory. Shallow water equations have been applied to model landslides and avalanches. In the process of applying these equations to model the different phenomena, some limitations may be encountered. Tough restrictions are put in place and an evaluation of the results obtained has to be done to verify their validity.
In the DG method the domain is discretized such that $J_i = [x_{i-\frac{1}{2}}, x_{i+\frac{1}{2}}]$ with $i = 1, 2, \cdots, N$ where N is the number of elements. Multiplying by the weight function $v(x)$ and integrating over the element J_i we have

$$\int_{x_{i-\frac{1}{2}}}^{x_{i+\frac{1}{2}}} [\mathbf{U}_t + \mathbf{F}(\mathbf{U})_{\mathbf{x}} - \mathbf{S}(\mathbf{U})] v(x) dx = 0$$

. We obtain for each element a weak formulation of the form

$$\int_{x_i-\frac{1}{2}}^{x_i+\frac{1}{2}} \xi \frac{\partial u}{\partial t} dx + f(u)\xi \Big|_{x_i-\frac{1}{2}}^{x_i+\frac{1}{2}} - \int_{x_i-\frac{1}{2}}^{x_i+\frac{1}{2}} f(u) \frac{\partial \xi}{\partial x} dx - \int_{x_i-\frac{1}{2}}^{x_i+\frac{1}{2}} s(u)\xi dx = 0$$

For each element the equation is integrated independently applying an explicit time-stepping scheme. The problem of dam fail may lead to huge economic loses. It may lead to loss of lives, damage to property and infrastructure. So, no matter how strong the dam has been built, the risk of breaking of the dam need to be assessed. This risk assessment is done in terms of; the depth of the flow and the velocities after the dam fails. A team of experts involved with downstream flood prediction and early warning systems in the case of a dam failure has to be put in place. Also, regular maintenance has to be carried on the dam so that its life can be increased. If the dam is left unmaintained, this exposes it to weakening and hence a possible failure. For example, if trees are left to grow near the dam, the dam may develop cracks due to penetration of roots into the embankments. Through leakage and flow of water through the cracks on the wall, the wall become eroded hence weakening. The main factors which lead to dam failure include;

i. natural factors such as flooding which may lead to excess water capacity in the dam.

ii. use of poor construction materials which wear out and weaken with time.

iii. cracking of the dam embankment caused by piping and internal erosion of soil in the embankment.

iv. inadequate maintenance services on the dam.

In the test/practical problem, we considered a representation of the water flow following a dam break using 1D SWE. The results obtained show a very close match with those obtained by P. Garcia-Navarro, A. Fras T. Villanueva, (1999) and Samir K. Das, Jafar Bagheri

(2015).
The discontinuous Galerkin finite element is suitable for models that involve hyperbolic PDEs. The non-linearity of the 1D shallow water equations used here results into a formation of a bore wave which propagates a finite speed within the domain. The discontinuous bases used in this method are suitable for such shock waves. We used Roe Riemann solvers to resolve the fluxes at the boundaries of the elements. These solvers accommodate the physics of wave propagation. The RK-TVD method is used to ensure that the approximated solution remains bounded in an arbitrary semi-norm $|w_h^n| \leq |w_h^0|, \forall n \geq 0$. This applies if the intermediate Euler steps, $w_h^{(l)} \longrightarrow v_h^{il}$, remains bounded at every intermediate step in this arbitrary in this arbitrary semi-norm, $|v_h^{il}| \leq |w_h^l|$. According to Cockburn *et al*, if degree 0 polynomials are used the DGFEM results in a monotone scheme and stability is ensured in the total variation semi-norm,

$$|v_h^n|_{TV} \leq |w_h^n|_{TV}$$

where the TV semi-norm is defined

$$|w_h|_{TV} = \sum_{i=1}^{N} |\bar{w}_{i+1} - \bar{w}_i|$$

The slope limiter used eliminates fast oscillations which are experienced near the shock fronts.

6.1.2 Recommendation

More work still remains undone in the field of SWE models and in the implementation of the solution methods. Following the results of this work, we would recommend further research on the following areas;

1. It is an advantage that the 2-dimensional ocean circulation SWE has been derived in chapter 2. This equation need to be solved using the RKDGFEM.
2. There is a need that the slope limiter used in the RKDG method be modified so that it can accommodate a varying bottom of the domain.
3. The RKDG method still leaves room for modification so that it will be able to handle moving boundaries. The boundary here changes due to flooding or drying. Thus aflooding and drying algorithm still remains to be determined.

Bibliography

[1] Harnet E., V. Legat and E. Deleersnijder, 2003. *A comparison of three finite elements shallow water equations.* Ocean modeling 5, (17-35)

[2] Hanert E., D. Y. Le Roux, V. Legat, E. Deleersnijder, 2003. *Advection schemes for unstructured grid modelling,* Ocean modelling 7, (39-58)

[3] Hanert E., D. Y. Le Roux, V. Legat, E. Deleersnijder, 2003. *Comparison of 4 advection schemes for use in unstructured grid ocean modelling.* Proceedings of the sixth national congress on Theoretical and Applied Mechanics, Ghent (Belgium), 8 pp

[4] A.J., C.N., Marshall, J.C., 1999. *A new treatment of the Coriolis terms in C-grid models at both high and low resolutions.,* Monthly weather Review 127:8, 1928-1936,

[5] Behrens J., 1998. *Atmospheric and ocean modelling with an adaptive finite element solver for the shallow water equations.* Applied Numerical Mathematics 26, (217-226)

[6] Mark A. Cane, *Introduction to Ocean Modeling*.

[7] Patrick Adrich, Gurvan Madec and Didier L'Hostis:, *Performance Evaluation for an Ocean General Circulation Model: Vectorization and Multitasking, In Proceedings 1988 International conference on Supercomputing, ACM,* St. Malo, France, July 1988, pp295-302.

[8] L.F. Richardson, *Weather prediction by Numerical Process,* Cambridge University Press, Cambridge, (1922) Introduction to Ocean Modeling)

[9] McDougall, T. J. (2003) *Potential Enthalpy: A conservative Oceanic variable for evaluating heat heat conted and heat fluxes.,* J. Phys. Oceanogr., 33 (945-963)

[10] McDougall, T. J. R.J. Greatbatch and Y. Lu (2003) *On conservation equations in oceanography: How accurate are Boussineq ocean models?,* J. Phys. Oceanogr., 32 (1574-1584)

[11] Hellberg R. W., and Adcroft A., 2006 *On methods of solving the oceanic equations of motion in generalized vertical coordinates,* Ocean Modelling, 11, (224-233)

[12] Arbic, B., Wallcraft, A., and Metzger, E. (2010),. *Concurrent simulation of the eddying general circulation and tides in a global ocean model.* Ocean Modelling, 32, (175-187)

[13] Bleck, R. (2002). *An oceanic general circulation model framed in hybrid isopycnic-cartesian coordinates.* Ocean Modeling, 4, (55-88)

[14] Brankart, J. M., (2013), *Impact of uncertainties in the horizontal density gradient upon low resolution global ocean modeling,* Ocean Modelling, Submitted

[15] A.J. Campin, J.M Hill, C.N. Marshall, *Implementation of an atmosphere-ocean general circulation model on the expanded spherical cube* .,Monthly weather review, 2004.

[16] Arakawa A. *Computational design for longterm numerical integrations of the equations of fluid motion: two-dimensional incompressible flow. Part I.* Journal of physics 1, 1996, 119-143.

[17] Behrens J., 1998. *Atmospheric and oceanic modelling with an adaptive finite element solver for shallow water equations.* Applied Numerical Mathematics 26, 217-226

[18] P.E. Bernard, N. Chevaugeon, V. Legat, E. Deleersnijder and J. F. Remacle. *High-order h-adaptive discontinuous Galerkin methods for ocean modeling.* Ocean Dynam., 2007.

[19] D. Blayo and L. Debren *Adaptive mesh refinement for finite difference ocean models first experiments.* J. Phys. Oceeanogr., 1999

[20] Blumberg A.F., and G.L. Mellor, *A description of three-dimensional Ocean circulation model, in Three-dimensional ocean circulation models, Vol. 4, edited* N. Heaps, pp 208, American Geophysical Union, Washington D.C. 1987.

[21] Blumberg A.F., and G.L. Mellor, *Diagnostic and Prognostic numerical circulation studies of the South Atlantin,* Bight J., Geophys. Res., 88, 4579-4592 (1983)

[22] Greatbatch, R.J., Y. Lu, and Y. Cai (2001), *Relaxing the Boussinesq approximation in Ocean Circulation Models,* J. Atmos. Ocean. Technol., 18 (1911-1923)

[23] Gregg, M., T. Sanford and D. Winkel (2003), *Reduced mixing from the breaking of internal waves in equatorial waters, Nature, 422,* (513-515)

[24] Griffies, S. M. (2005) *Some Ocean Model Fundamentals, in Ocean Weather Forecasting: an Integrated view of Oceanography,* Vol 577, edited by E. P. Chassignet, and J. Verron, pp 19-73, Springer, Berlin

[25] Tsunami Runuponto, a complex Three-dimensional Beach; Monai valley , *accassed 18-1-2017*

[26] Audusse E., Bouchut F., Bristeau M.O., Klein R. and Perthame B., *A fast and stable well-balanced scheme with hydrostatic reconstruction for shallow water flows,* SIAM J. Sci Comput., (2004), 2050-2065

[27] LeVeque R.J., *Balancing source terms and flux gradients in high resolution Gudonov methods: the quasi-steady wave-propagation algorithm,* J. Comput. Phys. 146 (1998), (346-365)

[28] LeVeque R.J., George D.L. and Berger M.J., *Tsunami modeling with adaptively refined finite volume methods,* Acta Numer. 20 (2011) 211-289

[29] Liu P.L.F., Yeh H. and Synolakis C., *Advances in Coastal and ocean Engineering,* World Scientific, (2008.)

[30] Chanson H., *The hydraulics of open channel flow,* Arnold, (1999)

[31] Vreugdenhill, C.B., *Numerical methods for shallow water flow,* Kluwer Ac.Pub., Dordrecht, The Netherlands, (1994.)

[32] Toro, E.F., *Shock capturing Methods for Free-surface shallow water flows,* John Wiley and sons, (2001)

[33] Burguete, J., Garcia-Navarro, P. *Efficient construction of high-resolution TVD conservatives schemes for equations with source terms: applications of shallow water flows,* International Journal for Numerical methods in Fluids, **37,** pp. 209-248, (2001)

[34] Brufau, P. and Garcia-Navarro, P., *Two-dimensional dam break flow simulation,* Int. J., for Num. Meth. Fluid dynamics **33**, pp. 35-57, (2000)

[35] Bleck, R., 2002, *An oceanic general circulation model framed in hybrid isopycnic-cartesian coordinates.* Ocean modeling 4, (55-88)

[36] G. Strang and G. J. Fix, *An analysis of the Finite element method,* Prentice Hall, (1973)

[37] C. Johnson, *Numerical solution of Partial Differential Equations by the Finite Element Method,* Cambridge University Press, (1980)

[38] S. C. Brenner and L. R. Scott, *The Mathematical Theory of Finite Element Methods,* Springer-Verlag, New York, (1994, Second edition 2002)

[39] *Fundamentals of the Finite Element Method for Heat and Fluid flow,* R.W. Lewis, P. Nithiarasu and K.N.Seetharamu. Wiley Ltd. (2004) ISBN: 0-470-84788-3

[40] Niels Ottosen and Hans Pettersen, *Introduction to the Finite Element Method,* Prentice, 1992, 1st Ed, 1992

[41] Dietrich Braess: *Finite Elements,* Cambridge, 3rd Ed, (2007)

[42] Bernado Cockburn and Wang Chi-Shu. *The Runge-Kutta discontinuous Galerkin method for conservation laws V: Multidimensional systems.* Technical Report TR-97-43, (1997)

[43] P. Jamet. *Galerkin-type approximations,which are discontinuous in time for parabolic equations in a variable domain.* SIAM J. Numer. Analy, 15 912-928 (1978)

[44] Toro E. Spruce M, Speares W. *Restoration of the contact surface in the HLL-Riemann solver,* Shoch Waves, (1994) 4(1): 25-34

[45] Ying X, Khan AA, Wang SSY. *Modelling Dam break flows using finite volume method on unstructured Grid.* Engineering Application of Computational Fluid Mechanics, 2009, 3(2): 184-194.

[46] Gotlieb S, Shu CW., *Total Variation diminishing Runge-Kutta schemes.* Mathematics of Computation, (1998); 67(221) 73-85

[47] Wu W., and Wang, S.S. (2007). *One-dimensional Numerical model for Nonuniform Sediment Transport under Unsteady Flows in Channel Networks,* Journal of hydraulic Engineering, 130(9) 914-923

[48] Ying X, Jorgeson J, Wang SSY (2009), *Modelling Dam-break flows using Finite volume methods on unstructured grid,* Engineering Applications of Computational Fluid Mechanics,3(2): 184-194

7 Appendix

7.1 MatLab Code for the Problem